



Surface Compositions of Trojan Asteroids

Joshua P. Emery¹ · Richard P. Binzel² · Daniel T. Britt³ · Michael E. Brown⁴ ·
Carly J.A. Howett^{5,6} · Audrey C. Martin³ · Mario D. Melita^{7,8} ·
Ana Carolina Souza-Feliciano^{3,9} · Ian Wong¹⁰

Received: 16 June 2023 / Accepted: 4 March 2024 / Published online: 25 March 2024
© The Author(s) 2024

Abstract

The Jupiter Trojan asteroids are a key population for understanding the chemical and dynamical evolution of the Solar System. Surface compositions of Trojans, in turn, provide crucial information for reconstructing their histories. NASA's *Lucy* mission will soon complete the first spacecraft reconnaissance of this population. This review summarizes the current state of knowledge of Trojan surface compositions and looks ahead to expected advances in that knowledge from *Lucy*. Surface compositions of Trojans remain uncertain due to a relative lack of diagnostic absorption features, though dedicated observations have begun to provide some clues to compositions. Trojans have uniformly low albedos, with a population average of $\sim 5.3\%$, and red spectral slopes at ultraviolet, visible, and near-infrared wavelengths. A bimodality of spectral slopes has been detected and confirmed across all these wavelengths, and the ratio of "less-red" to "red" Trojans increases with decreasing size. A broad absorption at $\sim 3.1 \mu\text{m}$ in some less-red Trojans may indicate the presence of N-H bearing material. Mid-infrared emissivity spectra reveal the presence of fine-grained anhydrous silicates on the surfaces. The meteorite collection contains no identifiable analogs to Trojan asteroids. Among small body populations, some Main Belt asteroids, comets, irregular satellites, and Centaurs provide reasonable spectral matches, supporting some genetic relationships among some members of these groups. The cause of the observed spectral properties remains uncertain, but recent suggestions include a combination of volatile ice sublimation and space weathering or a combination of impact gardening and space weathering. The *Lucy* mission will provide detailed compositional analysis of (3548) Eurybates, (15094) Polymele, (11351) Leucus, (21900) Orus, and (617) Patroclus-Menoetius, a suite of targets that sample the diversity among the Trojan population along several dimensions. With these flybys, the *Lucy* mission is poised to resolve many of the outstanding questions regarding Trojan surface compositions, thereby revealing how the Trojans formed and evolved and providing a clearer view of Solar System history.

Keywords Trojan asteroids · Asteroids · Lucy · Composition · Spectroscopy

1 Introduction

The Solar System is ever-changing, and changes were particularly rapid and dramatic in the early stages of its evolution. Spurred by observations of diverse planetary systems around

Extended author information available on the last page of the article

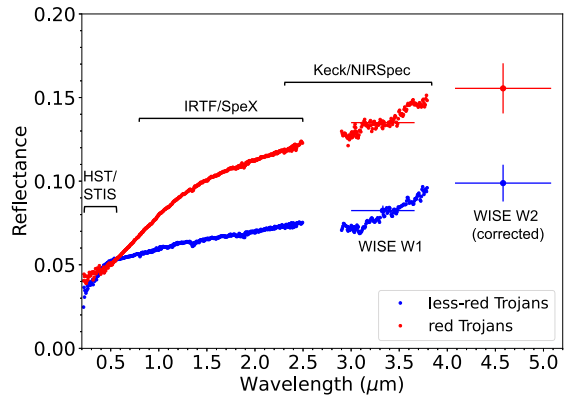
other stars as well as open questions about the Solar System, various styles and episodes of planet migration have been modeled for the Solar System. Small bodies (asteroids and comets) and their distribution across the Solar System are tracers of the original composition and thermochemical conditions in their formation regions, dynamical events (such as planet migration), and physical effects from interactions with the space environment. What we learn about the Solar System, the only planetary system we can study *in situ*, illuminates how other planetary systems evolve and how many of those, and which ones, may foster life.

The Trojan asteroids share Jupiter's orbit around the Sun, trapped in the L4 (leading) and L5 (trailing) stable Lagrange regions at ~ 5.28 AU. These 1:1 mean motion resonant orbits are stable over the lifetime of the Solar System (Levison et al. 1997). Marzari and Scholl (1998) showed that objects would be captured from the local population into the Lagrange regions as Jupiter grew. However, this capture mechanism does not explain the observed inclination distribution of Trojan asteroids. More recent works have alternatively proposed capture later in Solar System history, as part of the orbital migration of the giant planets in the Nice model (Tsiganis et al. 2005). Morbidelli et al. (2005) originally suggested that as Jupiter and Saturn smoothly migrate into a mean motion resonance with each other, any existing bodies are removed from the Lagrange regions, and as they migrate out of the resonance, a new population is captured (so-called chaotic capture). Nesvorný et al. (2013) demonstrated that bodies can also be trapped in Lagrange regions when Jupiter "jumps" (i.e., changes semi-major axis quickly) during close scattering of ice giant planets (so-called jump capture, as part of the jumping-Jupiter version of the Nice model) (Morbidelli et al. 2009). In any version of the Nice model, the captured Trojan population is dominated by bodies that were scattered from the Kuiper Belt, predicting that present-day Trojan asteroids originated in the Kuiper Belt.

Surface compositions of Trojan asteroids provide crucial information for reconstructing their histories. Nebular conditions in their formation region(s) set original compositions (e.g., silicate mineralogy, ices, and organics). Trojan asteroids are thought to be primitive, meaning their compositions have not been significantly altered since formation. Nevertheless, any internal heating that may have modified bulk compositions would be controlled by the original composition. Any potential surface modification by space weathering would also depend on the original surface composition as well as Trojan dynamical histories. Detailed compositional analysis of the suite of minerals, ices, and organics on the surface and in the near subsurface enables the unraveling of the complex influences to help establish evolutionary timelines. Comparisons with analog populations also provide key insights into present-day compositions and evolutionary histories of Trojan asteroids.

Several reviews of the surface compositions of Trojan asteroids have been published previously (Dotto et al. 2008; Slyusarev and Belskaya 2014; Emery et al. 2015). Here, we build on those reviews with a focus on advances in knowledge since their publication. We begin with an overview of the current state of knowledge of Trojan surface compositions, including insights gained from spacecraft and telescopic observations of other small body populations, and a discussion of potential mechanisms that can alter their surface compositions over time. We then describe outstanding questions regarding the surface compositions of Trojans and discuss how NASA's *Lucy* mission to provide the first up-close investigation of Trojans will address those questions.

Fig. 1 Average reflectance spectra of less-red and red Trojans from 0.2 to 5.0 μm , compiled from Emery et al. (2011), Grav et al. (2012), Brown (2016), and Wong et al. (2019a). The two subpopulations show distinct near-UV, optical, and near-infrared continuum slopes. Note the weak 3.1 μm absorption that is primarily observed on less-red objects



2 Observational Constraints on Surface Composition

2.1 Albedos

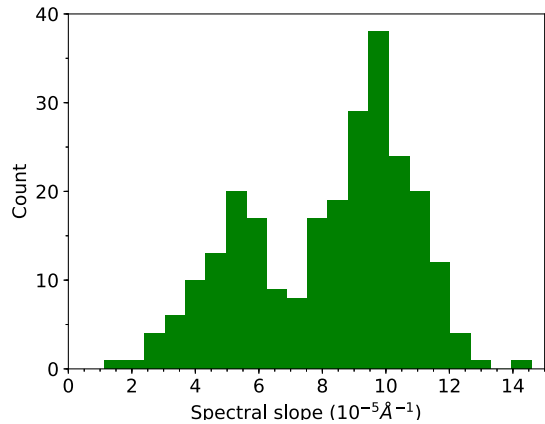
Compared to other populations of small bodies in the solar system, the albedos of the Trojan asteroids appear remarkably uniform and low. Analysis of thermal emission from the Wide-field Infrared Space Explorer (WISE) mission of 476 Trojan asteroids showed a mean V-band albedo of 6.9% — with only a small spread — for the largest, well-measured objects (Grav et al. 2012). Correcting these measurements using updated absolute magnitudes (Romanishin and Tegler 2018) drops the true albedos to a mean of only 5.3%. These low values are similar to those seen in dark cometary nuclei (Lamy et al. 2004).

While the largest Trojan asteroids appear uniformly low albedo, there is some evidence that smaller Trojans can have higher albedos. Fernández et al. (2009) measured thermal flux of 44 small (5 to 24 km) Trojans using the *Spitzer Space Telescope* and found that these small bodies had statistically higher albedos than larger Trojans. The WISE data show an upward trend of albedo for smaller diameters, but this trend can plausibly be attributed solely to the larger uncertainties for the smaller objects, known bias in absolute magnitudes for small objects, and the positive bias of albedo. Nonetheless, a small number of small well-measured WISE Trojans appear to have higher-than-typical albedos. Simpson et al. (2022) observed a subset of the WISE high-albedo objects with ALMA and also found that some ~ 20 –30 km Trojans have albedos as high as 13%. They hypothesized that these smaller objects contain evidence of recent catastrophic impacts which can — perhaps only briefly — give access to fresh interior material before it has been extensively space weathered.

2.2 Reflectance Spectrophotometry in the Ultraviolet, Visible, and Near-Infrared

Average reflectance spectra of Trojans from 0.2 to 5.0 μm are shown in Fig. 1. The earliest efforts to characterize the surface composition of Trojans through visible reflectance spectroscopy revealed featureless spectra with positive spectral slopes comparable to D-type asteroids in the outer Main Belt (Gradie and Veverka 1980). Subsequent visible spectroscopy throughout the following decades targeted a significant fraction of the large Trojans ($D > 50$ km), uncovering a wide range of spectral slopes — from neutral to moderately red — while continuing to yield no incontrovertible molecular absorptions (Jewitt and Luu 1990; Vilas et al. 1993; Bendjoya et al. 2004; Lazzaro et al. 2004; Fornasier et al. 2004; Dotto et al. 2006; Fornasier et al. 2007; Melita et al. 2008). Similarly, near-infrared

Fig. 2 Histogram of visible spectral slope for 293 Trojan asteroids observed by SDSS, showing the observed bimodality in color



spectroscopy through 2.5 μm has hitherto failed to detect any spectral features (Luu et al. 1994; Dumas et al. 1998; Emery and Brown 2003; Dotto et al. 2006; Yang and Jewitt 2007; De Luise et al. 2010; Emery et al. 2011; Marsset et al. 2014). Particularly notable is the lack of silicate and water ice features in the near-infrared spectra, which are otherwise quite common throughout the middle and outer Solar System. The absence of these prominent absorptions in spectra of Trojans has been a persistent mystery, given that water ice and silicates are expected to comprise much of the bulk composition of Trojans.

The advent of all-sky photometric surveys has greatly enriched our knowledge of Trojan reflectance spectra by enabling the study of population-level trends. The Sloan Digital Sky Survey (SDSS) imaged hundreds of Trojans in five photometric bands: u' (360 nm), g' (470 nm), r' (620 nm), i' (750 nm), and z' (890 nm). Analyses of the visible spectral slope distribution derived from SDSS photometry demonstrated that the Trojans have a bimodal color distribution (Fig. 2) (Szabó et al. 2007; Roig et al. 2008; Wong et al. 2014). The bimodality is attested in both the L4 and L5 swarms and does not appear to be correlated with any orbital parameter (Fornasier et al. 2007; Melita et al. 2008; Emery et al. 2011). Likewise, broadband near-infrared reflectance measurements obtained by the WISE mission in the W1 band (3.4 μm) showed a robust bifurcation among the largest Trojans in the sample (Grav et al. 2012). Further evidence of bimodal spectral characteristics comes from 0.7–2.5 μm spectroscopy of 68 Trojans observed using the Infrared Telescope Facility (IRTF; Fig. 1) (Emery and Brown 2003; Emery et al. 2011); the derived broadband near-infrared colors are clustered into two groups in $J - K$ vs. $0.85 - J$ space.

Crucially, when examining Trojans that are shared among the SDSS, WISE, and IRTF datasets, the respective bimodal classifications are consistent; i.e., objects belonging to the redder of the two visible color groups also have redder near-infrared colors and higher W1 reflectance, and vice versa (Wong et al. 2014). This observation indicates that the Trojan population as a whole contains two subpopulations, whose members differ systematically with respect to several spectral properties across the visible and near-infrared wavelength range and therefore must possess distinct surface compositions and/or regolith properties. These subpopulations are conventionally referred to as less-red and red. The *Lucy* mission targets are representative of the two subpopulations. (617) Patroclus-Menoetius and (15094) Polymele are in the less-red group, whereas (11351) Leucus and (21900) Orus are in the red group. (3548) Eurybates is an exception, with published spectral slopes from neutral (compatible with C-type asteroids) (Fornasier et al. 2007) to less-red (Souza-Feliciano et al. 2020; Emery et al. 2011).

The large body of visible colors provided by SDSS has allowed for the luminosity/size distributions of the less-red and red subpopulations to be characterized independently. The less-red and red luminosity distributions were shown to differ substantially. Specifically, the slope of the distributions are strongly divergent at intermediate sizes ($H \gtrsim 10$ or $D \lesssim 50$ km), with the fraction of less-red objects monotonically increasing with increasing H (decreasing size) (Wong et al. 2014). A follow-up wide-field photometric survey of small Trojans corroborated this finding by extending the attested trend to objects with diameters in the 1–10 km range and demonstrating that less-red objects dominate the Trojan population at the smallest sizes (Wong and Brown 2015). If Trojan albedos turn out to be systematically higher at smaller sizes (see Sect. 2.1), the observation of an increasing less-red fraction at small sizes would not change, though the size at which the transition from red-dominated to less-red dominated would be at a somewhat smaller size than noted in Wong and Brown (2015). Previously, Fornasier et al. (2007) found no trend in spectral slope from visible spectra of 142 Trojans in collisional families with $D > 16$ km. It is likely that the smaller sample size was not sufficient to resolve the trend in this size range observed in Wong and Brown (2015). Another notable finding concerns the Eurybates family — the only robustly attested collisional family in the Trojans (Brož and Rozehnal 2011): the collisional fragments do not display the color bimodality seen in the background population and are exclusively less-red (Fornasier et al. 2007). These two peculiar observations have broad implications for our understanding of Trojan surface composition (see Sect. 4).

Recently, spectroscopic characterization of Trojans has been extended into the near-ultraviolet (NUV). Reflectance spectra spanning 220–550 nm were obtained using the Hubble Space Telescope (HST) for six large Trojans, three from each color subpopulation (Wong et al. 2019a). The subpopulation-averaged ultraviolet spectra show distinct spectral shapes: namely, less-red objects (as characterized by visible color) have steeper NUV spectral slopes than red objects. Figure 1 summarizes the current state of our understanding of Trojan reflectance spectra from 0.2 to 5.0 μm . The subpopulation-averaged HST and IRTF spectra are combined with the averaged visible spectra from available literature sources, as well as the WISE broadband reflectances at W1 (3.4 μm) and W2 (4.6 μm). The differences in spectral shape between the less-red and red subpopulations are most evident at wavelengths less than ~ 2 μm . Humes et al. (2022) observed four of the *Lucy* targets (Patroclus, Eurybates, Leucus, and Orus) in the UV with HST. They did not find the same slope-trend reversal as Wong et al. (2019a), but they report a UV reflectance “bump” near 0.35 μm not detected in the Wong et al. (2019a) data. They interpret the UV bump as Rayleigh scattering by sub-micron-sized opaque grains.

2.3 3–5 μm Spectra

Ground-based reflectance spectroscopy of these faint bodies is difficult beyond 2.5 μm and has only been obtained for a handful of the brightest objects (Cruikshank et al. 2001; Emery and Brown 2003; Brown 2016), though WISE observations obtained photometry in the W1 (3–4 μm) and W2 (4–5 μm) bands of many objects (Grav et al. 2012). The spectra and WISE photometry show that the reflectance of both the less-red and red Trojans continues to rise approximately linearly through at least 5 μm (Fig. 1).

Cruikshank et al. (2001) and Emery and Brown (2003) report no absorptions in this wavelength range outside of the noise in the spectra. Emery and Brown (2004) use those non-detections to place limits of a few percent on abundances of water ice and hydrated silicates on Trojan surfaces and slightly higher limits on complex organic molecules. They also suggest that the lack of strong organic features indicates that the red VNIR slopes cannot be due to organics, as previously suggested.

Brown (2016) report an absorption at 3.1 μm in several large Trojans, with a strong anti-correlation with color. Absorptions in these regions are often attributed to fine-grained water ice, but such grains would quickly be depleted on the surfaces of these objects, so unusual circumstances such as recent collisions would be required for water ice to be present. The appearance of this feature on all of the less-red objects observed makes this explanation unlikely. The absorption could perhaps be explained as part of an N-H stretch feature at 3.13 μm . Beyond the 3.1- μm absorption, additional absorptions appear, consistent with organic materials that might be expected on objects such as these. In the ground-based data, these appear strongest on the least-red of these objects. Unfortunately, with the low signal-to-noise of these data, little definitive can be said about the species responsible for these absorptions beyond 3 μm .

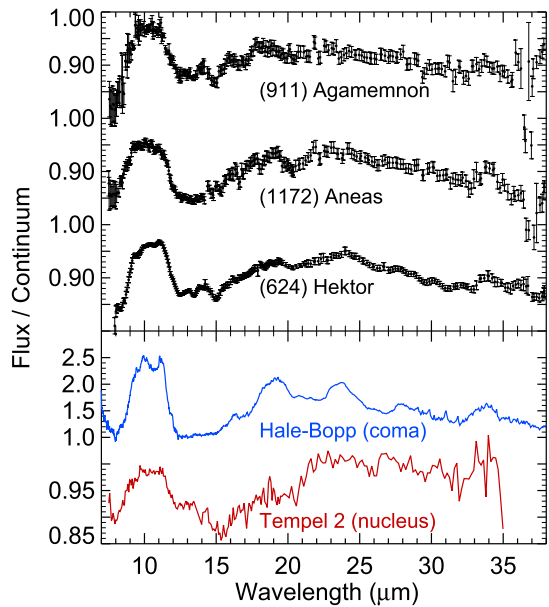
2.4 Mid-Infrared Emission Spectroscopy

The first Mid-Infrared (MIR; 5–30 μm) spectra of Trojan asteroids looked at (624) Hektor, (1172) Aneas, and (911) Agamemnon taken with the Spitzer Space Telescope (SST) (Emery et al. 2006). The spectra reveal a broad 10- μm emissivity feature with a spectral contrast of roughly 10–15% along with two smaller and broader peaks near 19 and 24 μm (Fig. 3). The spectra of these three Trojans are indicative of fine-grained crystalline silicates, such as olivine and pyroxene. The shape and spectral contrast bear a resemblance to that of comets, for which optically thin comae result in strong 10- μm emission features when comprised of fine-grained ($\lesssim 10 \mu\text{m}$) disperse silicates. Trojans do not have comae (e.g. Perna et al. 2018b), so researchers hypothesize that the emissivity peaks arise from a fluffy (i.e. highly porous) regolith of fine grain silicates, or from silicates suspended in a transparent matrix (Emery et al. 2006; Vernazza et al. 2012; Yang et al. 2013). Through comparisons of the SST spectra to laboratory spectra of olivine and pyroxene mixed with potassium bromide salt to simulate regolith porosity, Martin et al. (2022, 2023a) conclude that the regolith porosity on Hektor is in excess of 80%. Using T-Matrix and Hapke spectral modeling, Lowry et al. (2022) obtain similar results, including a likely olivine-rich silicate component. Martin and Emery (2023) present MIR spectra of 11 additional Trojans measured with SST, and all show similar emissivity peaks indicative of fine-grained silicates. The red spectral group have larger spectral contrasts in the 10- μm plateau than the less-red group.

Subsequent MIR observations of the Patroclus-Menoetius system with the SST revealed spectra that look similar to that of Hektor (Mueller et al. 2010). The Patroclus spectrum has a well-defined 10- μm feature, though the spectral contrast is about half that of Hektor's 10- μm feature, and a perceptible feature near 20 μm . As with the other three Trojans, Patroclus likely contains fine-grain crystalline silicates on its surface. Though Hektor belongs to the spectrally red group, and Patroclus belongs to the spectrally less-red group, their similar MIR spectra suggest a compositional similarity, at least for the silicate component.

In addition to the crystalline silicates on Trojan surfaces observed in the MIR, there are likely contributions from amorphous and opaque materials. Patroclus and Aneas have rounded 10- μm emissivity features, as opposed to a trapezoidal 10- μm feature seen in Hektor's spectrum (Kelley et al. 2017; Martin 2022; Martin and Emery 2023). Rounded emission features can be explained by amorphous silicates or hydrated silicate spectra (Lisse et al. 2006; Harker et al. 2007; Kelley and Wooden 2009; Izawa et al. 2021). No indications of hydration have been detected at either 0.7 μm or $\sim 3 \mu\text{m}$ on Trojans, but amorphous silicates would be expected on bodies that formed in the outer Solar System (e.g. Henning 2010). The MIR spectral contrasts of all four Trojans are much less than that of comets or laboratory studies of analog material (Izawa et al. 2021; Martin et al. 2022, 2023a). Additional

Fig. 3 MIR emissivity spectra of (1172) Aneas, (911) Agamemnon, and (624) Hektor, from Emery et al. (2006). Spectra of the coma of comet Hale-Bopp (blue; Crovisier et al. 1997) and the nucleus of comet Tempel 2 (red; Kelley et al. 2017) are shown for comparison (see Sect. 3.3). The Trojan and Tempel 2 nucleus spectra are shown at the same scale, but note the significant difference in scale factor for Hale-Bopp



material, such as amorphous carbon or opaques (e.g., FeS), reduce the spectral contrasts of emission features in the MIR and are featureless in the VNIR (e.g. Hanner et al. 1994; Wooden et al. 2004; Wooden 2008; Woodward et al. 2015). Non-compositional factors may also contribute to the decreased spectral contrast, such as larger grain sizes or lower surface porosity compared to comets.

2.5 Thermophysical Properties

Thermal inertias based on thermophysical modeling of thermal infrared observations have been reported for only a few Trojan asteroids. Fernández et al. (2003) measured simultaneous visible and multi-band infrared (12.5 and 20.8 μm) fluxes of 9 Trojan asteroids, from which they derived an average beaming parameter of 0.94. Arguing that such a low beaming parameter indicates a “slow rotator” thermal model ($\Theta < 1$, where $\Theta = \Gamma \sqrt{\omega} / \epsilon \sigma T_{ss}^3$, Γ is thermal inertia, ω is rotation rate, ϵ is bolometric emissivity, σ is the Stefan-Boltzmann constant, and T_{ss} is sub-solar temperature) applies to the Trojans, they computed an upper limit to the thermal inertia of $\sim 50 \text{ J m}^{-2} \text{ K}^{-1} \text{ s}^{-1/2}$, similar to the Moon and large Main Belt asteroids. Applying similar arguments to the results for WISE observations of Trojans reported by Grav et al. (2012), in which beaming parameters for nearly all of the 478 Trojans reported are < 1 , would suggest that low thermal inertias are common among Trojan asteroids.

Emery et al. (2006) mention that thermophysical models of infrared spectra (5.2 to 38 μm) of the three Trojans in Fig. 3 provide upper limits of $\sim 50 \text{ J m}^{-2} \text{ K}^{-1} \text{ s}^{-1/2}$ on the thermal inertias of those three large Trojans. Mueller et al. (2010) report thermal inertias of 21 ± 14 and $6.4 \pm 1.6 \text{ J m}^{-2} \text{ K}^{-1} \text{ s}^{-1/2}$ for the two components of the 617 Patroclus binary from heating and cooling curves measured with SST infrared spectral observations of shadowing during mutual events. Horner et al. (2012) computed a thermal inertia of 25 to $100 \text{ J m}^{-2} \text{ K}^{-1} \text{ s}^{-1/2}$ (3σ confidence range) for the dynamically unstable Trojan 1173 Anchises from thermophysical modeling of IRAS, AKARI, and WISE thermal photometry.

These low thermal inertia values reported for Trojan asteroids suggest dusty, porous surfaces, consistent with the thermal infrared emissivity spectra discussed in Sect. 2.4. Such low thermal inertias appear common on moons of the giant planets, Centaurs, and Kuiper Belt Objects (e.g. Müller et al. 2020, and refs therein) and indicate that fine-grained regoliths are common in the outer Solar System.

3 Analogs

3.1 Meteorites

Meteorite analogs provide useful insight into the surface composition of asteroids. Interestingly, there are no meteorite analogs that have been confidently identified for the enigmatic Trojans. The Tagish Lake Meteorite was initially touted as a spectral analog for D-type asteroids based on the relatively steep VNIR spectral slope, although it displays a 3- μm absorption feature (e.g. Hiroi et al. 2001) not observed in spectra of Trojans. Emery et al. (2006) and Vernazza et al. (2013) found that the MIR spectrum of Tagish Lake meteorite powder (Hiroi et al. 2001; Roush 2003) is a poor match to the emission spectra of the large Trojans Hektor, Aneas, and Agamemnon, and Vernazza et al. (2013) also demonstrated that the VNIR reflectance spectrum of Tagish Lake is also a poor match to VNIR Trojan spectra. Despite the incompatibility between Tagish Lake and Trojans, Vernazza et al. (2013) found a good spectral match at all wavelengths between Tagish Lake and the Main Belt D-type asteroid 368 Haidea, indicating compositional variability among D-type asteroids. Searches within meteorite spectral databases such as ASTER,¹ which includes carbonaceous chondrites, ordinary chondrites, and enstatite chondrites, among others, return no good matches to the observed Trojan emissivity spectra (Emery et al. 2006).

To broaden the possibilities in identifying meteorite analogs for Trojan asteroids, Vernazza et al. (2012) measured chondrite powder diluted with KBr in the MIR and found similarities to the Hektor emission spectra. KBr salt is transparent in the MIR, which results in the diluted meteorite grains appearing well separated in this wavelength regime. Similar experiments were later performed with additional meteorites such as Tagish Lake and ordinary chondrites (Izawa et al. 2021), as well as terrestrial olivine and pyroxene minerals (Martin et al. 2022, 2023a). Regardless of Tagish Lake dilution, its spectra deliver a poor match to any Trojan emission spectra. However powdered ordinary chondrites and powdered olivine spectra produce similar spectra to the Trojans, particularly Hektor, when diluted with KBr.

3.2 Main Belt and Near-Earth Asteroids

In plotting the heliocentric distribution of asteroid taxonomic classes Gradie and Tedesco (1982) showed the predominance of low albedo and red-sloped P- and D-type asteroids in the outer belt and Trojan populations. Ongoing spectral surveys have solidified these findings, showing that strong representations of these classes are also included in the Cybeles (7:4 resonance at 3.5 AU) and the Hildas (3:2 resonance at 4 AU) (Grav et al. 2012; DeMeo and Carry 2013; Wong and Brown 2017b). Nevertheless, D-types have been detected among small members of the inner and middle Main Belt as well (e.g. Lazzaro et al. 2004; DeMeo et al. 2014). Bourdelle de Micas et al. (2022) also found 3 D/T types among relatively large (D~30 to 50 km), likely primordial planetesimals in the inner Main Belt (~4% of their

¹<http://speclib.jpl.nasa.gov/>

measured sample). The identification of D-types across the Main Belt suggests scattering of D-types into the innermost parts of the Solar System at some point during its evolution. In their spectral modeling of a large data set of D-type spectra, Gartelle et al. (2021) found that Main Belt D-types appear to contain a higher abundance of opaque minerals than Trojans.

Low albedo and D-type members are also well known in the near-Earth population (Fernández et al. 2001; Binzel et al. 2004; Perna et al. 2018a). The majority of these objects are very highly correlated with Jovian Tisserand parameter values less than 3, indicating a dynamical link and origin associated with Jupiter Family Comets (see Sect. 3.3). However, not all D-types found in the near-Earth and Mars-crossing populations have a viable dynamical link to the outer belt or Jupiter Family comet source regions (Carry et al. 2016; Binzel et al. 2019). The existence of NEA D-types sourced from the inner and middle Main Belt emphasizes that although D-types are predominantly located in the outer belt and Trojan swarms, some D-type material has been scattered more broadly.

The only low-albedo Main Belt object that has been visited by a spacecraft is the dwarf planet Ceres. Although Ceres is a differentiated C-complex body with a disk-averaged VNIR spectrum that is very different from Trojan spectra and absorption features in the 3–4- μm region that are also distinct from Trojans (e.g. Rivkin et al. 2022), insights from its evolution have some relevance to understanding Trojans. NASA's *Dawn* mission found an average surface composition on Ceres rich in hydrated and ammoniated clays and carbonates (De Sanctis et al. 2015; Ammannito et al. 2016), indicating widespread heating and alteration of the original materials. The presence relatively large amounts of nitrogen, as expressed in the widespread occurrence of ammoniated clays, has been attributed to an outer Solar System origin for Ceres (e.g. Ribeiro de Sousa et al. 2022), though the nitrogen may be consistent with typical CM/CI chondrite bulk composition (McSween et al. 2018). In any case, the *Dawn* results highlight that searches for nitrogen-bearing materials on Trojans are important for comparisons with other bodies and for assessing formation region. Spectral mapping by the *Dawn* mission also revealed significant surface heterogeneity not indicated by disk-integrated spectra, including substantial exposures of H_2O ice, complex organic material, and salts, providing important clues to and constraints on interior composition and passed geologic activity (e.g. Combe et al. 2016; De Sanctis et al. 2017; de Sanctis et al. 2018; De Sanctis et al. 2020). By analogy, spectral mapping of Trojans is likely to provide a clearer view of interior compositions and any past activity than disk-integrated spectra alone.

3.3 Comets

The Nice Model predicts that Trojans are dynamically linked to outer Solar System Kuiper belt objects (KBOs) and are therefore related to Jupiter Family Comets (JFCs; Morbidelli et al. 2005). JFCs, such as 9P/Tempel, have comae made primarily of H_2O , CO_2 , and sub-micron sized silicate grains (Farnham et al. 2007; Feaga et al. 2007; Harker et al. 2007). Ices have not been observed on Trojan surfaces (Emery and Brown 2003; Yang and Jewitt 2007; Brown 2016), but the observed silicates can be useful for comparisons to comets.

Typically, silicate-rich comae are dominated by amorphous phases (Wooden 2002; Kelley and Wooden 2009), although crystalline silicates have been detected (e.g. Harker et al. 2005; Sugita et al. 2005; Watanabe 2004; Lisse et al. 2006; Harker et al. 2007). The silicate phase (i.e., amorphous vs. crystalline) is also instructive for understanding the condition and region of formation. The crystalline fraction of silicates (f_{crist}) is typically used in comet research to investigate high-temperature processing that formed dust in the inner disk of the solar nebula (Bockelée-Morvan et al. 2002; Ciesla 2007; Hughes and Armitage 2010). In general, minerals that formed in the inner solar nebula were transported outward and mixed with amorphous dust grains prior to forming a comet (Charnoz and Morbidelli 2007).

Another parameter of silicate composition that can be used to compare Trojans and comets is the $Mg/(Mg+Fe)$ value of olivine and pyroxene, which has been used to constrain the structure and evolution of circumstellar dust (Hanner et al. 1994; Tielens et al. 1998; Gail and Sedlmayr 1999). Silicates in the solar nebula trended from more Mg-rich crystalline silicates in the inner Solar System to Fe-rich silicates in the outer Solar System. In the MIR, as $Mg/(Mg+Fe)$ decreases, emissivity peaks associated with olivine and pyroxene shift from shorter to longer wavelengths (Koike et al. 1993; Jäger et al. 1998; Chihara et al. 2002; Koike et al. 2003).

Trojans' highly porous surfaces, evidenced by strong emissivity peaks (see Sect. 2.4), coupled with red-sloped reflectance spectra (see Sect. 2.2) and low thermal inertia (see Sect. 2.5), makes comets a useful analog, despite Trojans' lack of comae (Perna et al. 2018b). Generally, comet nuclei fall under D-type classification in the VNIR (see Sect. 2.2), and, in the MIR, comet nuclei emission spectra bear similarities to Trojans (Kelley et al. 2017) (Fig. 3). The fine-grained material on the surface of comet nuclei is primarily made of Mg-rich silicates, intermediate Mg/Fe silicates, and carbonaceous and metal sulfide material (e.g. Frank et al. 2014; Wooden 2002). Currently, the JFC 10P/Tempel 2 is the prime cometary spectral analog to Hektor (Kelley et al. 2017), suggesting that other red (D-type) Trojans should have a similar silicate makeup of fine-grained Mg-rich and Mg/Fe mixed silicates.

The JFC 67P/Churyumov-Gerasimenko was observed in exquisite detail by the European Space Agency (ESA) *Rosetta* spacecraft. Despite being an active comet, disk-averaged spectra of the nucleus do not show H_2O , though local exposures of H_2O are observed in color and spectral mapping data (e.g. Pommerol et al. 2015; De Sanctis et al. 2015; Barucci et al. 2016; Fornasier et al. 2016; Deshapriya et al. 2018; Fornasier et al. 2023), and H_2O was exposed in boulders contacted by the Philae lander (O'Rourke et al. 2020). Observed exposures range in size from about 1 to over 1500 m² and have lifetimes from a few hours (for frosts) to more than two years. After sublimation, these regions became indistinguishable from the surrounding dark and red terrain. The many observations of H_2O exposures and their distribution indicate that H_2O is abundant below the surface (e.g. Fornasier et al. 2016, 2023; Oklay et al. 2017). These observations are consistent with *Deep Impact* spacecraft observations of the nucleus of the JFC 9P/Tempel 1 (Sunshine et al. 2006) and suggest that Trojans could have H_2O beneath their surfaces, even though no spectral signatures have been detected in disk-integrated telescopic data. Localized exposures of CO_2 ice were also detected in resolved spectra of 67P (Filacchione et al. 2016), highlighting the possibility of more volatile ices also being masked by dusty regoliths.

Spectra of the low-albedo material covering the nucleus of 67P show a broad $\sim 3.1\text{-}\mu\text{m}$ absorption that has been interpreted as ammonium salts (Poch et al. 2020). This feature is distinct from the ammoniated clay feature detected on Ceres, but still indicates significant nitrogen, highlighting again the importance of searches for nitrogen-bearing materials on Trojans. Complex organic molecules also likely help explain the broad $\sim 2.9\text{-}$ to $3.6\text{-}\mu\text{m}$ absorption on 67P (e.g. Capaccioni et al. 2015; Quirico et al. 2016), and aliphatic organics have been detected in the dark material (Raponi et al. 2020).

3.4 Irregular Satellites

The Nice Model predicts that the irregular satellites of the giant planets were captured in the same scattering event and from the same Kuiper Belt source population as the Trojan asteroids (Morbidelli et al. 2005). Graykowski and Jewitt (2018) find that the average visible colors of the irregular satellites of all four giant planets are statistically consistent with each

other and that they lack the ultra-red colors seen among the Kuiper Belt, though the small number of Uranian and Neptunian irregulars weaken the statistics for those groups. The average colors of Jupiter and Saturnian irregulars are consistent with the average colors of Trojan asteroids, though the Jupiter irregulars contain more neutral-sloped (C-type) surfaces than the Trojans. Bottke et al. (2010) argue that the irregular satellite populations were once much larger and have been extensively ground down from collisions. If irregular satellites and Trojans have less-red or neutral interiors (e.g. Wong and Brown 2016) (see Sect. 4.1), this larger abundance of neutral-sloped surfaces may be a result of the enhanced collisional environment. Interestingly, Graykowski and Jewitt (2018) point out that the similarity of average colors of the irregulars at different distance from the Sun (and therefore different surface temperatures) and distinct color distributions from KBOs argue against a thermal process at 5 AU causing the difference in colors between Trojans and their presumed KBO source population.

Our closest view of what a Jupiter Trojan asteroid would look like *before* being heated to the temperatures of the Jupiter region comes from Saturn's irregular satellite Phoebe. Phoebe was presumably captured from solar orbit early in the history of the Solar System and now resides on a distant inclined orbit about Saturn. Phoebe is only a little smaller than Hektor, the largest Jupiter Trojan, so could be a model for a less-heated version of a large Trojan.

Phoebe's albedo of about 8% (Buratti et al. 2008) is relatively low, but a bit higher than the average for Trojans. Phoebe's average VNIR spectrum is spectrally neutral (Owen et al. 1999), distinct from those of Trojans, though some regions have slightly red spectral slopes (Buratti et al. 2008). Near infrared spectroscopy reveals, distinct absorption features due to water ice on the surface of Phoebe (Owen et al. 1999; Clark et al. 2005). Images and spectra from Cassini reveal that Phoebe's surface is dominated by large impact basins (Porco et al. 2005) and that the water ice spectral features, though present everywhere, are strongest in these regions of impact (Clark et al. 2005; Buratti et al. 2008; Fraser and Brown 2018). Overall, the surface appears to be water ice poor but with impacts revealing an icier interior. While water ice is not stable for long periods of time at the current temperatures of the Trojans, the overall low albedo with high albedo patches showing on Phoebe in regions of impacts is similar to what is inferred from the presence of higher albedo small Trojans that might have had recent impacts (see Sect. 2.1).

3.5 Centaurs

Centaurs are an enigmatic population of minor bodies with orbits that traverse the giant planet region. Dynamical studies have shown that these objects are inward-scattered KBOs and are characterized by orbital stability lifetimes on the order of 1–10 Myr (Tiscareno and Malhotra 2003; Horner et al. 2004). Given their formation location in the outer Solar System and relatively close present-day heliocentric distances, Centaurs have attracted a great deal of interest as proxies for studying the more distant KBOs and may represent bodies in a transition from KBO-like to Trojan-like surfaces.

Over the past few decades, observational studies have uncovered several similarities between Centaurs and Jupiter Trojans. The most salient common trait is color bimodality. Centaurs have been shown to display bifurcations in both visible (Peixinho et al. 2003; Tegler et al. 2003, 2008, 2016) and near-infrared (Delsanti et al. 2006) colors. In the following, we refer to the two color classes in the Centaurs and KBOs as red and very-red. Notably, the color centers of the two Centaur sub-populations lie at redder spectral slope values than the two color groups in the Trojans. Red Trojans have similar slopes as red Centaurs, and

very red Centaurs have no analog in the Trojan population. Given the dynamical history of Centaurs, it had long been suggested that this color bimodality is indicative of two broad color classes in the wider KBO population (Fraser and Brown 2012; Peixinho et al. 2012, 2015; Tegler et al. 2016), a scenario that has been confirmed by recent photometric survey observations of similarly-sized KBOs (Wong and Brown 2017a; Schwamb et al. 2019).

Another important similarity between Centaurs and Trojans is very low geometric albedos. However, whereas the less-red and red Trojans have similar albedo distributions, the Centaur sub-populations differ significantly in their reflectivity: the median albedos of the red and very-red groups are 5% (similar to the average for Trojans) and 11%, respectively (Duffard et al. 2014; Romanishin and Tegler 2018; Müller et al. 2020). Median albedos of most dynamical groups of KBOs are higher than those of Trojans (Müller et al. 2020). One exception is the Scattered Disk Objects (SDOs), which have a median albedo of $\sim 6\%$, though the spread of albedos is much higher among the SDOs. If Trojans are scattered KBOs, it would not be surprising that their albedos are systematically lower from loss of ices that are common on KBOs. Likewise, the two Centaur sub-populations are characterized by discrepant inclination distributions, with the very-red objects having lower inclinations on average (Tegler et al. 2008; Romanishin and Tegler 2018). The emissivity spectrum of the red Centaur Asbolus is very similar to those of red Trojans (Barucci et al. 2008), suggesting similar surface texture and silicate mineralogy (see Sect. 2.4).

With their origins in the outer Solar System, Centaurs are expected to be rich in volatile ices. Near-infrared spectroscopy of several Centaurs, including Chiron, Pholus, Thereus, and Chariklo, has revealed absorption signatures of water ice (Brown and Koresko 1998; Cruikshank et al. 1998; Romon-Martin et al. 2003; Licandro and Pinilla-Alonso 2005; Barkume et al. 2008; Stansberry et al. 2008; Duffard et al. 2014). In addition, methanol ice has been detected on four objects, including Pholus and Crantor (Cruikshank et al. 1998; Stansberry et al. 2008; Duffard et al. 2014). The volatile-rich nature of Centaurs is also manifested by the peculiar subset of objects that show cometary activity (Jewitt 2009). Comae have been observed on Centaurs at heliocentric distances greater than 12 AU (Tegler et al. 2006; Bauer et al. 2008; Jewitt 2009, 2015) — far beyond the region where water ice sublimates — which indicates that the activity is primarily driven by a different physical process, perhaps the crystallization of amorphous ice or sublimation of more volatile ices (Prialnik et al. 1995; Jewitt 2009; Guilbert-Lepoutre 2012). Notably, the color distribution of active Centaurs is skewed toward bluer colors when compared to the inactive population (Jewitt 2009, 2015; Wong et al. 2019b), suggesting that the activity may be altering the primordial colors of Centaurs. Analogous bluing of colors due to activity was observed on the nucleus of comet 67P by the *Rosetta* mission (e.g. Fornasier et al. 2016, 2023; Ciarniello et al. 2022).

The advent of dynamical instability models of solar system evolution and the proposed outer Solar System origin of Trojans have made comparisons between Centaurs and Trojans particularly apropos. Numerical models simulating the dynamical instability show that some planetesimals from the primordial trans-Neptunian protoplanetary disk were initially scattered onto highly-eccentric Centaur-like orbits before being captured into resonance by Jupiter to become Trojans (Morbidelli et al. 2005; Nesvorný et al. 2013). Therefore, detailed study of Centaurs may further our understanding of how the combined effects of increased solar irradiation and cometary activity could have affected the surface properties of Trojans in the early Solar System.

4 Compositional Interpretation and Surface Evolution

4.1 Theoretical and Observational Considerations

Of the observational constraints discussed in Sect. 2, the color bimodality is perhaps the most consequential observational constraint on compositional models of Trojans. Broadly speaking, the disparate spectral properties of less-red and red Trojans suggest one of two possible scenarios: (1) less-red and red Trojans were formed in different locations and have distinct bulk compositions, or (2) all Trojans were initially formed in the same environment and accreted an identical bulk composition, with the bifurcation in spectral properties arising from different sublimation and evolutionary histories that affect only the ices retained in the near surface and the surface regolith. Current models of Solar System evolution largely align with the second scenario, with the Trojans forming in the outer Solar System alongside the progenitors of the present-day Kuiper belt and Centaurs, before being scattered inward and captured into resonance during an episode of dynamical instability sometime after the dispersal of the protoplanetary disk. It follows that in order to reconcile the observed surface properties of Trojans with these dynamical models, a mechanism must be invoked to create two distinct surface chemistries from a common bulk composition.

One hypothesis posits that volatile ice sublimation and space weathering may be the primary drivers behind the observed Trojan color bimodality (Wong and Brown 2016) and also behind the color and spectral diversity in the Kuiper Belt (e.g. Schaller and Brown 2007). Within the framework of dynamical instability models of Solar System evolution, all bodies that formed in the planetesimal disk beyond the primordial orbits of the ice giants would have accreted a roughly cometary composition, i.e., rocky material and water ice, with a significant volume of other volatile ices such as carbon dioxide, methanol, and ammonia. When the protoplanetary disk dissipated, these objects were exposed to direct insolation, resulting in sublimation of volatile ices in the outermost layers. After millions of years of exposure, the strongly temperature-dependent, and by extension heliocentric-distance-dependent, sublimation rates produced distinct surface ice compositions across the primordial icy planetesimal disk, while keeping the interior bulk composition unchanged (e.g. Schaller and Brown 2007; Steckloff et al. 2021).

Simple sublimation modeling has demonstrated that hydrogen sulfide ice (H_2S) is conditionally unstable to sublimation loss at these heliocentric distances and could therefore be the critical volatile ice species responsible for the development of the color bimodality. Objects in the planetesimal disk would have been divided into two groups — the objects situated closer to the Sun experienced higher surface temperatures and became depleted of H_2S on their surfaces, while objects farther out retained H_2S . The retention of H_2S , which is known to induce a strong reddening upon irradiation (Carlson et al. 2007), would contribute additional reddening relative to the case where H_2S is absent. The result of space weathering on these two distinct surfaces is the development of a color bimodality among objects in the primordial planetesimal disk: less-red objects without surface H_2S , and red objects with surface H_2S . The subsequent dynamical instability spread these bodies throughout the Solar System to become the present-day Trojans, KBOs, and Centaurs, which thereby inherited the color bimodality. Other simple ices also redden upon irradiation (e.g., CH_3OH and CH_4), but their volatilities are such that their sublimation lines would not have bifurcated the original Kuiper Belt like H_2S would.

This hypothesis explains the color bimodality attested across all middle and outer solar system minor body populations. In addition, it naturally accounts for the less-red Eurybates collisional family, as well as the broader trend of increasing less-red fraction with decreasing size. Since the physical and chemical processes responsible for the bifurcation in color

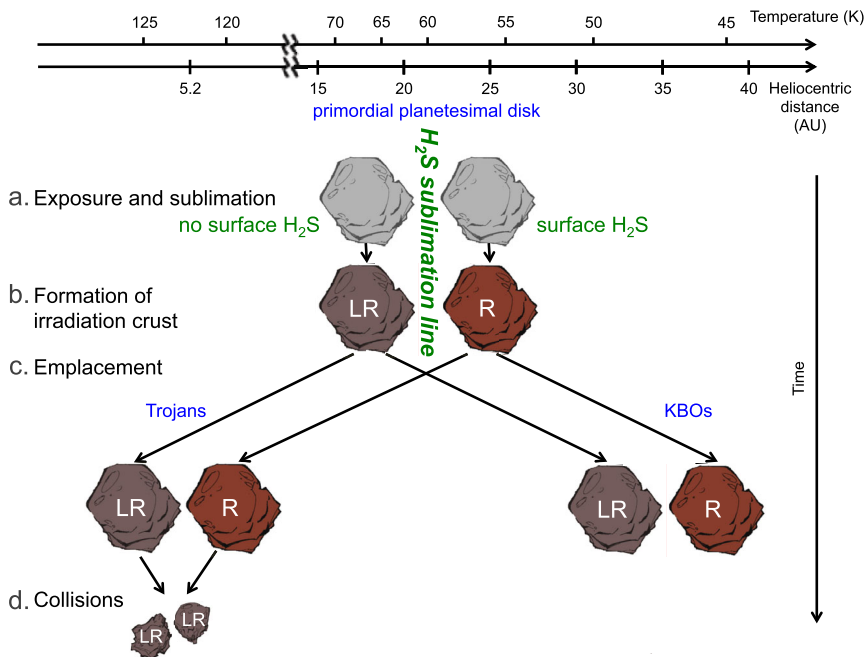


Fig. 4 Schematic diagram illustrating the H₂S ice sublimation hypothesis proposed by Wong and Brown (2016) to explain the color bimodality of Jupiter Trojans and KBOs. Primordial planetesimals that were situated on two sides of the H₂S sublimation line attained different levels of reddening depending on the loss or retention of H₂S ice on their surfaces

are confined to a thin outer irradiated shell, collisions readily destroy this crust, exposing the pristine interior material. At the much higher surface temperatures of the present-day Trojans, any remaining volatile ices would instantaneously sublimate away. In particular, H₂S, the reddening species responsible for the development of red objects, would be depleted in all cases, and subsequent irradiation of the fragments would only produce less-red colors. The various features of the H₂S ice sublimation hypothesis are illustrated in Fig. 4.

4.2 Laboratory Studies

Motivated by the aforementioned H₂S sublimation hypothesis (Wong and Brown 2016), a laboratory study was carried out with a focus on the irradiation of volatile ices of relevance to the Jupiter Trojans (Mahjoub et al. 2016, 2017; Poston et al. 2018). Samples consisting of water, ammonia, and methanol ices, with or without the inclusion of H₂S ice were subjected to high-energy electron bombardment at temperatures representative of the primordial planetesimal disk and then heated to Trojan temperatures. The experimental methodology was designed to simulate the initial space weathering of Trojans in the outer Solar System and the subsequent thermophysical evolution that transpired during the transition to their current environment.

Notably, the results of the experiments reproduce many of the general observed features of Trojan asteroids. Both samples reddened and darkened upon electron bombardment, accompanied by the formation of an irradiation mantle on the surface. The sample with H₂S attained a steeper spectral slope throughout the visible and near-infrared, consistent with the

hypothesized role of sulfur irradiation chemistry in creating the redder colors of red Trojans. In addition, spectral slope was reduced in both samples upon subsequent heating to Trojan-like temperatures, suggesting that secondary thermal processing of the surface regolith upon emplacement into their present-day orbits may have led to the more neutral colors of Trojans when compared to Centaurs and KBOs.

Detailed compositional analysis of the irradiation residues revealed the production of short-chain sulfur allotropes S_2 , S_3 , and S_4 , which have been previously shown to induce strong reddening in laboratory samples. These allotropes are unstable to heating and can further polymerize to form longer sulfur chains such as S_8 that are characterized by more neutral visible spectra. High-resolution reflectance spectroscopy of the samples also uncovered a series of narrow absorptions at wavelengths longer than $3 \mu\text{m}$, including several sulfur-bearing molecules (e.g., OCS, CS_2 , and SO_2) only detected in the sample with H_2S . Future high-precision spectroscopic observations with facilities like the *James Webb Space Telescope* (JWST) may be able to probe for some these diagnostic absorption features, which will definitively test the sulfur hypothesis for the Trojan color bimodality.

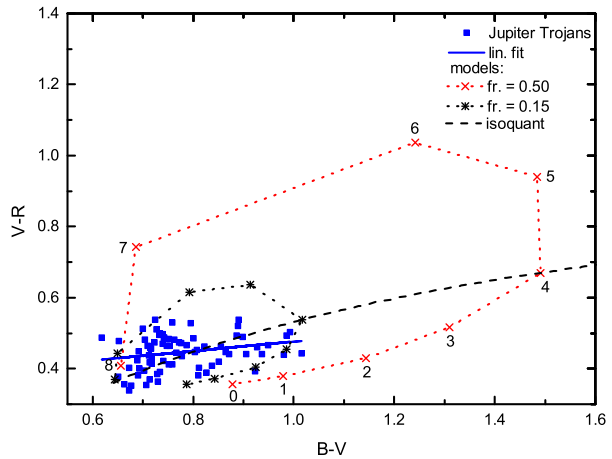
4.3 Space Weathering and Collisional Processes

Even if a genetic relationship with the hot classical KBOs is established, differences between their surface properties are to be expected due to the different evolution of the two populations in their different environments. The major processes responsible for modifying the surfaces are space weathering (e.g., irradiation by solar ions, galactic cosmic rays, electrons, UV, and X-rays) and/or physical collisions with other minor bodies or micrometeorites. How a surface is altered by these processes depends on chemical composition, the rate of the process, and on the location in the Solar System.

The most studied space-weathered airless body is the Moon, where the most prominent effect is the formation of nano-phase iron (npFe). Inclusion of npFe in glassy rims coating surface grains causes the reflectance spectra to become redder (i.e., increasing the spectral slope) and lowers the albedo (see for example Hapke 2001). In the case of S-type asteroids, as parent bodies of ordinary chondrite meteorites, a reddening trend has also been established (Binzel et al. 2004). These trends have been validated in the laboratory with similar results for different weathering agents, since both ion irradiation and laser irradiation/ablation experiments produce on the silicates reddening and darkening spectral trends (Hapke 1965; Moroz et al. 1996; Sasaki et al. 2001; Strazzulla et al. 2005; Marchi et al. 2005; Brunetto et al. 2006; Loeffler et al. 2008, 2009; Fu et al. 2012). On darker objects, such as C-type asteroids, the evidence is more controversial – weak reddening trends have been observed by some investigators (Lazzarin et al. 2006), while other studies have found a blueing effect (Nesvorný et al. 2005; Lantz et al. 2013; Vernazza et al. 2013).

A review of space weathering experiments performed on terrestrial and extraterrestrial materials can be found in Brunetto et al. (2015), which can be briefly summarized as follows. On high albedo materials, such as olivine, both ion and laser irradiation produce strong spectral reddening and darkening. Similar, but weaker, effects occur for pyroxenes. On low albedo terrestrial bitumens, a very strong spectral flattening and a weak brightening trend is produced. On organic residues of C-rich ices, a spectral reddening and darkening is produced due to the formation of refractory molecular solid materials, and a similar trend is observed for organics covering silicates. Irradiation experiments of carbonaceous chondrite meteorites show that the CV and CO groups darken and redden, like ordinary chondrites, olivine, and pyroxene, whereas CI and CM groups brighten and become bluer. It is unclear whether the different behaviors are caused by organic content (low vs high), silicate composition

Fig. 5 V-R vs. B-V color indexes of the Jupiter Trojans from the MBOSS database. Color change of the model Trojan for different surface fraction of the “polystyrene phase”. The isoquant that better reassembles the linear fit of the data is plotted



(anhydrous vs hydrated), or chondrule abundance (relatively higher vs lower) (Lantz et al. 2017).

Several attempts have been made to assess the combined effect of space weathering and the rejuvenation of the surface by impact gardening. It has been noted that water ice is very short lived on the surface of a Jovian-Trojan due to rapid sublimation (Guilbert-Lepoutre 2014). Melita et al. (2009) postulated a bulk composition in which fresh sub-surface material is spectrally red dust. Under very specific circumstances, they found that the timescale for resurfacing the entire surface of the Trojan asteroids is similar to that of the flattening of the red spectrum of the new dust by solar-proton irradiation. Under such circumstances, the surfaces of most Trojan asteroids might be composed mainly by lowly irradiated (red) dust. This model would predict that smaller bodies, which are more likely to have suffered recent impacts, would be predominantly red-sloped, opposite to the trend described in Sect. 2.2.

As an analog to silicate grains coated in organic material, Kaňuchová et al. (2010) investigated the effect of irradiation of polystyrene-coated olivine. Polystyrene exhibits a progressive spectral reddening and then darkening during irradiation. At high irradiation doses, the reddening reaches a maximum, while the sample continues to darken and starts to flatten. Interestingly, the spectral shape of the irradiated material at different doses can reproduce some asteroid spectra. On the basis of these experimental results, a reddening-blueing loop has been proposed by Kaňuchová et al. (2012): Irradiated organics, initially exhibiting a flat spectrum and a high albedo, are progressively reddened while the albedo decreases. At very high doses, the spectra are flattened (blueing) while the albedo continues to decrease. A fully weathered organic will then have a flat and dark spectrum. In Melita et al. (2015), a model is constructed in which the surface is composed of two phases: one with constant albedo and spectral slope and one that evolves in the color-color diagram due to irradiation as polystyrene deposited on olivine, described in Kaňuchová et al. (2010). The color evolves due to irradiation along the reddening-blueing loop described by Kaňuchová et al. (2010), with a magnitude that is controlled by the relative initial amounts of the two components (see Fig. 5). The Trojan color distribution is best represented by a fraction of the organic-rich component of $\sim 15\%$ and an albedo of 0.04 for the other component. However, the timescale of surface rejuvenation implied by this model is unrealistically short, of only 100 yr.

The added contribution of cratering leads to irradiated less-red objects becoming red objects, once again through resurfacing, thereby preventing all the red Trojans from turning

into less-red objects of lower albedo. However, the characteristic collisional timescale and, correspondingly, the timescale of resurfacing increase with decreasing asteroid size because of the decreasing number of impactors that can reset the surface (Melita et al. 2015), while the rate of irradiation is the same for all objects, as mentioned earlier. Therefore, the resurfacing of Trojans through cratering becomes less effective at returning irradiated less-red objects to red objects when one goes to smaller sizes. This would lead to a relative excess of less-red objects at faint magnitudes, but it would imply a lower albedo for highly processed small objects, which does not coincide with the observations. In any case, these models based on the evolution of polystyrene deposited on olivine (Kaňuchová et al. 2010) under cosmic irradiation would not predict a bimodal distribution of colors but a smooth gradient.

5 Synthesis and Outstanding Questions

Dedicated telescopic observations, as discussed in Sect. 2, have begun to reveal the nature of this pivotal population. Generally, Trojans are dark, reddish objects with featureless spectra from the near-ultraviolet through 2.5 μm . Although albedos are uniformly clustered around 5%, VNIR spectral slopes are bimodal, with the ratio of less-red to red slopes increasing with decreasing size. The lack of any discernible water ice absorption between 1 and 4 μm places strong upper limits on the water ice abundance in the uppermost layers of the regolith. The spectral feature at $\sim 3.1 \mu\text{m}$ observed in spectra of some less-red Trojans has an ambiguous interpretation, as it can be attributed to either fine-grained water frost or a N–H vibrational absorption. MIR thermal emission spectra of Trojans show spectral features indicative of fine-grained silicates in a highly porous (i.e., “fluffy”) regolith.

Despite these important discoveries, several fundamental questions remain regarding the surface compositions of Trojan asteroids that confound a full understanding of their origin and evolution. Whereas fine-grained silicates have been detected, the mineralogy, chemistry, and crystalline fraction of these silicates, and whether these properties vary significantly among the population, remain uncertain. On primitive bodies, these silicate properties are indicative of nebular formation region. It is also important to establish the hydration state of silicates on Trojan asteroids in order to assess whether these bodies have undergone past heating events, either geothermal or impact-related.

The abundance and composition of organic materials is another significant unknown. The red spectral slopes of Trojans were initially interpreted to be due to abundant organic materials, but no clear organic absorptions have been detected. Characterization of organic molecules and comparisons to those on surfaces of KBOs will inform the origin and surface processing undergone by Trojans. The detection of N–H-bearing material is intriguing, and it will be illuminating to determine if that material is similar to the materials detected on Ceres or on comet 67P Churyumov-Gerasimenko. Of particular interest will be assessing whether that material is indicative of an outer Solar System origin, as suggested for Ceres and 67P.

The absence of H₂O absorptions from all Trojan spectra is something of a mystery. Bulk densities derived from binary orbits among Trojans are close to 1 g cm⁻³, suggesting a significant fraction of interior ice. Thermal stability studies show that H₂O ice can be stable within 1 to 10 m of the surface of Trojans (Guilbert-Lepoutre 2014). Spacecraft spectra of the surfaces of active comets have shown that interior ice is effectively masked, even while sublimation is occurring, by a dusty surface layer (see Sect. 3.3). Nevertheless, with high quality published NIR spectra of dozens of Trojans, one might expect to have seen some recent exposure of interior ice from recent large impacts, even considering that Earth-based

telescopic measurements yield spatial resolutions that are just hemispherical averages. It remains to be demonstrated whether interior ice is present and was lost from the surface by sublimation.

One of the biggest current open questions about Trojan asteroids is the cause of the observed color bimodality. The two scenarios in Sect. 4 discuss different possible paths, one due to different formation regions and the other due to surface processing, for a fundamental chemical difference between the red and less-red material. Determining the compositions of the two spectral groups is critical for distinguishing these scenarios. A specific question to assess the Wong and Brown (2015) scenario is whether the red material shows a sulfur-rich composition, and a question related to the Melita et al. (2015) model is whether either spectral class is consistent with the organic material suggested in that model. On the other hand, it is not even clear whether the bimodality is due to a chemical difference between the red and less-red material, or if a physical difference in the regoliths (e.g., grain size, regolith porosity) could cause the bimodality. A key to understanding the bimodality is determining whether fresh material is red or less-red, or if the fresh material itself is bimodal in composition.

It is also critical to determine how Trojan surfaces evolve due to space weathering. Many analyses invoke different styles, pathways, and timescales for surface alteration due to exposure to the space environment, but there are few constraints. It is not known whether one spectral group evolves from the other, or if the two surface types evolve differently. Along with determining surface composition of fresh and evolved materials, understanding space weathering requires determining the rate of alteration by irradiation compared to the rate of collisional resurfacing for Trojans of different size. Along with assessing the current ongoing space weathering evolution, it is necessary to unravel how Trojan surfaces were altered as they migrated from their presumed Kuiper Belt origin region to their present location. Trojans exhibit several observational differences from KBOs, Centaurs, and irregular satellites, and it is necessary to determine whether these differences can be explained by the changing thermal and irradiation environment that they experienced due to their orbital migration to Jupiter's Lagrange regions.

A theme that runs through all these open questions relates to potential regional scale variation in surface compositions on individual Trojans. The Trojan population as a whole exhibits less heterogeneity than almost any other Solar System small body population, yet Trojans are almost always inferred to have surfaces that are in some ways distinct from their interiors, due to a combination of sublimation, irradiation, and impact gardening. If this distinction between interior and surface is correct, individual Trojans should show regional and local scale variations in composition from exposures of fresh material and perhaps from differing irradiation doses of surfaces exposed for different amounts of time. If geothermal and/or impact-related hydration has occurred, one might also expect those processes to lead to regional scale variations in composition. Since telescopic observations observe entire hemispheres, it is difficult to assess surface exposures, unless a hemispheric-scale event has occurred. All told, deciphering surface compositions of Trojan asteroids is clearly dependent on spacecraft observations providing high spatial resolution of surface heterogeneities. With spatial resolution providing geologic context, we can hope to unravel which (if any) of the currently envisioned processes are active in the outer solar system.

6 How the Lucy Mission Will Address These Outstanding Questions

The *Lucy* mission is designed to address these outstanding questions related to surface composition and thereby reveal not only the histories of Trojan asteroids, but key aspects of the

evolution of the Solar System (Levison et al. 2021; Olkin et al. 2021). Levison et al. (2021) presents the Level 1 requirements of the *Lucy* mission and describes the broad science motivation for these requirements. The flyby targets sample the different Trojan spectral classes, sizes, binarity, rotation rate, shape, etc, enabling investigation of the compositional diversity of Trojans along multiple dimensions (see Table 3 and Fig. 7 of Levison et al. 2021), satisfying requirement 1 (R1) of the mission. As mentioned in Sect. 2.2, Orus and Leucus are in the red spectral group, Patroclus-Menoetius and Polymele are in the less-red group, and Eurybates is the largest member of a collisional family with neutral to less-red spectral slopes. Patroclus-Menoetius is a nearly equal-sized binary, and Eurybates and Polymele both have small moons. Rotation periods range from 8 hrs (Eurybates) to 445 hrs (Leucus), and shapes derived from light curve and occultation analyses (e.g. Mottola et al. 2023; Buie et al. 2021; Pinilla-Alonso et al. 2022) range from spheroidal (Patroclus-Menoetius) to elongate with significant topography (Leucus).

Instrumentation on the *Lucy* spacecraft is optimized for detecting materials than are critical for understanding the origin and evolution of Trojans (R12 and R13 of the mission). The Linear Etalon Imaging Spectral Array (LEISA) mapping spectrometer spectral range (1.0–3.6 μm), spectral resolution ($\Delta\lambda \sim 0.01 \mu\text{m}$), and sensitivity will enable detection of ices, organics, salts, and crystalline silicates of differing compositions (Olkin et al. 2021; Reuter et al. 2023). On approach and departure, low spatial resolution spectra will be obtained of each target over a full rotation period, spaced no more coarsely than 1/6 of a rotation period (R14) in order to map global-scale variations on the targets. Nearer the close approach, LEISA's spatial resolution of $\sim 40 \text{ m}$ at a distance of 500 km will map compositional heterogeneity, including fresh exposures of sub-surface materials (mission requirement R14).

The Multi-spectral Visible Imaging Camera (MVIC) will image the targets through 5 color filters (violet 377–489 nm; green 478–525 nm; orange 522–632 nm; phyllosilicate 627–758 nm; and NIR 753–914 nm) (Olkin et al. 2021; Reuter et al. 2023). The phyllosilicate filter is designed to search for the 0.7 μm absorption feature in Fe-bearing phyllosilicates. Approach and departure low spatial resolution images covering a full rotation spaced no more coarsely than 1/6 of a rotation period will map global-scale color variations (mission requirement R9). During the flybys, MVIC's higher spatial resolution ($\sim 15 \text{ m}$ at a distance of 500 km) will enable color imaging that covers 80% or $\geq 700 \text{ km}^2$ of each target capable of resolving features $\leq 1.5 \text{ km}$ in size, to characterize regional-scale compositional variations (mission requirement R10). Nearer to close approach, MVIC will obtain color images covering $\geq 150 \text{ km}^2$ capable of resolving features $\leq 600 \text{ m}$ in size, to characterize regional-scale compositional variations (mission requirement R11), including freshly exposed materials (Olkin et al. 2021; Reuter et al. 2023).

The highest spatial resolution images from the *Lucy* LORRI Range Reconnaissance Imager (L'LORRI) panchromatic visible camera ($\sim 3 \text{ m}$ at a distance of 500 km) will provide necessary geologic context for interpreting compositional heterogeneity and an understanding of the crater and resurfacing histories of Trojans (Olkin et al. 2021; Weaver et al. 2023). Measurements of thermal emission by the *Lucy* Thermal Emission Spectrometer (L'TES) point spectrometer (6–50 μm ; spatial resolution² $\sim 3.6 \text{ km}$ at a distance of 500 km) at multiple times of day, including at least one night time spot, will provide insights into surface structure and volatile stability (mission requirement R17) (Olkin et al. 2021; Christensen et al. 2024). For the warmest parts of the surfaces of each target, the SNR of the L'TES

²85% encircled energy.

images may be high enough to search for and interpret spectral features (e.g., of surface silicates), but thermal emission spectroscopy is not a requirement of the *Lucy* mission.

The majority of questions regarding the current surface composition of Trojans will be directly answered by spectra measured by LEISA. The abundance and composition of organics will be assessed primarily the 3–3.6 μm segment of measured spectra. Aliphatic organics have diagnostic features at ~ 3.4 and $3.5 \mu\text{m}$, aromatics have features near $3.3 \mu\text{m}$, and specific composition and structural details affect the shapes and positions of these features. N-H-bearing materials detected on other Solar System objects (e.g., ammoniated clays on Ceres and ammonium salts on comet 67P) are identified by relatively broad absorptions near $3.1 \mu\text{m}$. Potential N-H features have been detected in ground-based spectra of some less-red Trojans, albeit with fairly low S/N, and LEISA spectra will enable more detailed compositional analyses of these features to determine whether the materials are similar to those on Ceres or 67P or distinct from either. Hydrated minerals, diagnostic of past geothermal heating and aqueous alteration, have strong features near $2.7\text{--}2.9 \mu\text{m}$, the exact position of which is indicative of composition and therefore degree of alteration. The MVIC filter centered near $0.7 \mu\text{m}$ is designed to search for Fe-bearing hydrated silicates. Crystalline anhydrous silicates, such as olivine and pyroxene, exhibit broad absorptions near 1 and $2 \mu\text{m}$. H_2O ice has a strong, broad fundamental absorption near $3 \mu\text{m}$ as well as weaker overtone and combination absorptions at 1.5 and $2.0 \mu\text{m}$ that, together, will enable very sensitive searches for H_2O as well as characterization of the phase of any detected.

The overriding benefit of sending spacecraft to explore the Trojan asteroids is getting spatially resolved data. The *Lucy* mission will obtain rotationally-resolved global color and spectral data of the Trojan targets on approach and/or departure in order to assess regional-scale color and compositional variations. Color and compositional variations at regional scales will provide important constraints on large-scale geologic and internal thermal processes. Closer in, higher resolution color and spectral data will be obtained of smaller regions to investigate local variations, particularly those that might be due to exposures of fresh subsurface material. Analysis of compositional variations at different spatial scales is critical for addressing several of the most important outstanding questions. A search for H_2O ice in fresh exposures is important for answering whether H_2O was originally present in the bulk composition and was lost from the surface layer due to sublimation. Though the spatial resolutions expected for LEISA and MVIC during the Trojan flybys would not resolve the smallest H_2O exposures seen by *Rosetta* on the nucleus of comet 67P, it is sufficient to identify the larger exposures. Comparing the colors and compositions of fresh, subsurface material to surface layers exposed to the space environment will directly address how the surfaces of these bodies are space weathered. It is critical to understand whether the fresh material corresponds to the average red Trojans, the average less-red Trojans, or something else. Compositional signatures of weathered versus unweathered material will provide an understanding of the chemical processes involved in space weathering. Searching for sulfur-bearing materials in the fresh exposures will provide a key test of the Wong and Brown (2016) hypothesis for the color evolution of Trojans. Compositional and color analyses of surface and subsurface materials are also key to understanding the processing that may have occurred as Trojans migrated from the Kuiper Belt, answering why they currently look so different from KBOs.

Another key aspect of the design of the *Lucy* mission for addressing the outstanding compositional questions is that the spacecraft will flyby targets of different spectral classes and sizes. Comparison of the detailed color and compositional analyses at different spatial scales for the red (Orus and Leucus), less-red (Patroclus-Menoetius and Polymele), and neutral-sloped (Eurybates) Trojans is crucial for understanding whether the different classes

have different original compositions or are just weathered differently. An important focus will be determining how similar (or different) freshly exposed material on the different spectral classes is, and what the specific compositions of those materials are. The compositions of fresh material on the different bodies should trace back to formation region(s).

Information gained about surface geology (e.g. Marchi et al. 2023), internal properties (e.g. Mottola et al. 2024), activity (e.g. Noll et al. 2023), and collisional history (e.g. Bottke et al. 2023) will also provide important context for interpreting surface compositions. For example, collisional resurfacing rates on Trojans of different size control, compared to space weathering rates, control whether disk-integrated colors of large Trojans or small Trojans should appear fresher. This information, in turn, informs how the population-level trends of surface colors (see Sect. 4.1) should be interpreted. Mass and density determinations enabled by the close *Lucy* flybys, in particular, will provide important constraints on bulk composition to be compared with the surface composition. The suite of observations to be obtained by the *Lucy* mission analyzed together will revolutionize our understanding of the Trojan asteroids and the Solar System.

A JWST cycle 1 GO program (2574) has measured NIR and MIR spectra of all *Lucy* Trojan targets. The Near-InfraRed Spectrograph (NIRSpec) obtained 1.7 to 5.1 μm spectra of all 5 targets with the medium resolution grism. The Mid-InfraRed Instrument (MIRI) has obtained 5 to 28 μm spectra with the medium resolution grism of all 5 targets. These JWST data are much higher quality than possible from ground-based or even previous space-based facilities. The NIRSpec data show a $\sim 3.1\text{-}\mu\text{m}$ feature in the less-red targets, similar to that reported by Brown (2016), as well as some possible organic absorptions near 3.4 μm , which are deepest in the red targets (Wong et al. 2023). Eurybates also shows an absorption near 4.2 μm similar to features seen in the dark material of the large, regular moons of Jupiter and Saturn and attributed to complexed CO_2 . The MIRI data show 10- μm emissivity plateaus in all objects, consistent with previous MIR observations of Trojans (Martin et al. 2023b). Detailed analysis of these high quality spectra will provide the standard by which *Lucy* spectral data will be analyzed.

7 Conclusions

The Trojan asteroids remain poorly understood in terms of composition, yet those compositions would provide key constraints on Solar System evolution. Trojan's featureless VNIR spectra have long confounded attempts to investigate compositions. Broad absorptions near 3.1 μm in spectra of several less-red Trojans may be due to N-H-bearing materials, which could suggest an outer Solar System origin. MIR emissivity peaks near 10 and 20 μm indicate the presence of fine-grained silicates that appear to be similar in composition to cometary silicates. There are no good Trojan analogs among the meteorite collection, prohibiting similar insights that meteorites provide for many Main Belt asteroids. Placing Trojans in context with Main Belt asteroids, comets, irregular satellites of the giant planets, and Centaurs indicates some potential genetic relationships among at least some members of these disparate groups.

Bimodal spectral groups among the Trojans and the changing fractions of these groups with object size provide important clues to the evolution of Trojans. Hypotheses that rely solely on space weathering to explain colors fail to predict the spectral bimodality. One model that fits current data, put forth in Wong and Brown (2016), posits that the difference between the two groups is not original composition, but the stability of sulfur-bearing ices at different heliocentric distances in the early Kuiper Belt. NASA's *Lucy* mission is poised

to reveal the first views of the surfaces of Trojan asteroids. The detailed measurements of ices, organics, and silicates at different spatial scales on the diverse set of *Lucy* targets will answer the question of what the surface and bulk compositions of Trojans are, how the Trojans formed and evolved, and what their evolution tells us about Solar System history.

Acknowledgements We are grateful to the reviewer for comments and suggestions that improved the manuscript.

Declarations

Competing Interests The authors declare no competing interests.

Open Access This article is licensed under a Creative Commons Attribution 4.0 International License, which permits use, sharing, adaptation, distribution and reproduction in any medium or format, as long as you give appropriate credit to the original author(s) and the source, provide a link to the Creative Commons licence, and indicate if changes were made. The images or other third party material in this article are included in the article's Creative Commons licence, unless indicated otherwise in a credit line to the material. If material is not included in the article's Creative Commons licence and your intended use is not permitted by statutory regulation or exceeds the permitted use, you will need to obtain permission directly from the copyright holder. To view a copy of this licence, visit <http://creativecommons.org/licenses/by/4.0/>.

References

- Ammannito E, DeSanctis MC, Ciarniello M et al (2016) Distribution of phyllosilicates on the surface of Ceres. *Science* 353(6303):aaf4279. <https://doi.org/10.1126/science.aaf4279>
- Barkume KM, Brown ME, Schaller EL (2008) Near-infrared spectra of centaurs and Kuiper belt objects. *Astron J* 135(1):55–67. <https://doi.org/10.1088/0004-6256/135/1/55>
- Barucci MA, Brown ME, Emery JP et al (2008) Composition and surface properties of transneptunian objects and centaurs. In: Barucci MA, Boehnhardt H, Cruikshank DP et al (eds) *The solar system beyond Neptune*. University of Arizona Press, Tucson, pp 143–160
- Barucci MA, Filacchione G, Fornasier S et al (2016) Detection of exposed H₂O ice on the nucleus of comet 67P/Churyumov-Gerasimenko. As observed by Rosetta OSIRIS and VIRTIS instruments. *Astron Astrophys* 595:A102. <https://doi.org/10.1051/0004-6361/201628764>. arXiv:1609.00551 [astro-ph.EP]
- Bauer JM, Choi YJ, Weissman PR et al (2008) The large-grained dust coma of 174P/Echeclus. *Planet Space Sci* 120(866):393. <https://doi.org/10.1086/587552>
- Bendjoya P, Cellino A, Di Martino M et al (2004) Spectroscopic observations of Jupiter Trojans. *Icarus* 168(2):374–384. <https://doi.org/10.1016/j.icarus.2003.12.004>
- Binzel RP, Rivkin AS, Stuart JS et al (2004) Observed spectral properties of near-Earth objects: results for population distribution, source regions, and space weathering processes. *Icarus* 170(2):259–294. <https://doi.org/10.1016/j.icarus.2004.04.004>
- Binzel RP, DeMeo FE, Turtelboom EV et al (2019) Compositional distributions and evolutionary processes for the near-Earth object population: results from the MIT-Hawaii near-Earth object spectroscopic survey (MITHNEOS). *Icarus* 324:41–76. <https://doi.org/10.1016/j.icarus.2018.12.035>. arXiv:2004.05090 [astro-ph.EP]
- Bockelée-Morvan D, Gautier D, Hersant F et al (2002) Turbulent radial mixing in the solar nebula as the source of crystalline silicates in comets. *Astron Astrophys* 384(3):1107–1118. <https://doi.org/10.1051/0004-6361:20020086>
- Bottke WF, Nesvorný D, Vokrouhlický D et al (2010) The irregular satellites: the most collisionally evolved populations in the solar system. *Astron J* 139(3):994–1014. <https://doi.org/10.1088/0004-6256/139/3/994>
- Bottke WF, Marschall R, Nesvorný D et al (2023) Origin and evolution of Jupiter's Trojan asteroids. *Space Sci Rev* 219(8):83. <https://doi.org/10.1007/s11214-023-01031-4>. arXiv:2312.02864 [astro-ph.EP]
- Bourdelle de Micas J, Fornasier S, Avdellidou C et al (2022) Composition of inner main-belt planetesimals. *Astron Astrophys* 665:A83. <https://doi.org/10.1051/0004-6361/202244099>
- Brož M, Rozehnal J (2011) Eurybates - the only asteroid family among Trojans? *Mon Not R Astron Soc* 414(1):565–574. <https://doi.org/10.1111/j.1365-2966.2011.18420.x>. arXiv:1109.1109 [astro-ph.EP]

- Brown ME (2016) The 3–4 μm spectra of Jupiter Trojan asteroids. *Astron J* 152(6):159. <https://doi.org/10.3847/0004-6256/152/6/159>. arXiv:1606.03013 [astro-ph.EP]
- Brown ME, Koresko CD (1998) Detection of water ice on the centaur 1997 CU₂₆. *Astrophys J Lett* 505(1):L65–L67. <https://doi.org/10.1086/311593>
- Brunetto R, Romano F, Blanco A et al (2006) Space weathering of silicates simulated by nanosecond pulse UV excimer laser. *Icarus* 180(2):546–554. <https://doi.org/10.1016/j.icarus.2005.10.016>
- Brunetto R, Loeffler MJ, Nesvorný D et al (2015) Asteroid surface alteration by space weathering processes. Univ Ariz Press, pp 597–616. https://doi.org/10.2458/azu_uapress_9780816532131-ch031
- Buie MW, Keeney BA, Strauss RH et al (2021) Size and shape of (11351) Leucus from five occultations. *Planet Sci J* 2(5):202. <https://doi.org/10.3847/PSJ/ac1f9b>
- Buratti BJ, Soderlund K, Bauer J et al (2008) Infrared (0.83–5.1 μm) photometry of Phoebe from the Cassini visual infrared mapping spectrometer. *Icarus* 193(2):309–322. <https://doi.org/10.1016/j.icarus.2007.09.014>
- Capaccioni F, Coradini A, Filacchione G et al (2015) The organic-rich surface of comet 67P/Churyumov-Gerasimenko as seen by VIRTIS/Rosetta. *Science* 347(6220):aaa0628. <https://doi.org/10.1126/science.aaa0628>
- Carlson RW, Kargel JS, Douté S et al (2007) Io's surface composition. In: Lopes RMC, Spencer JR (eds) *Io after Galileo: a new view of Jupiter's volcanic moon*, Springer, Berlin, p 193. https://doi.org/10.1007/978-3-540-48841-5_9
- Carry B, Solano E, Eggl S et al (2016) Spectral properties of near-Earth and Mars-crossing asteroids using Sloan photometry. *Icarus* 268:340–354. <https://doi.org/10.1016/j.icarus.2015.12.047>. arXiv:1601.02087 [astro-ph.EP]
- Charnoz S, Morbidelli A (2007) Coupling dynamical and collisional evolution of small bodies. II. Forming the Kuiper belt, the Scattered Disk and the Oort Cloud. *Icarus* 188(2):468–480. <https://doi.org/10.1016/j.icarus.2006.11.018>
- Chihara H, Koike C, Tsuchiyama A et al (2002) Compositional dependence of infrared absorption spectra of crystalline silicates I. Mg-Fe pyroxenes. *Astron Astrophys* 391(1):267–273. <https://doi.org/10.1051/0004-6361:20020791>
- Christensen PR, Hamilton VE, Mehall GL et al (2024) The Lucy Thermal Emission Spectrometer (L'TES) Instrument. *Space Sci Rev* 220(1):1. <https://doi.org/10.1007/s11214-023-01029-y>
- Ciarniello M, Fulle M, Raponi A et al (2022) Macro and micro structures of pebble-made cometary nuclei reconciled by seasonal evolution. *Nat Astron* 6:546–553. <https://doi.org/10.1038/s41550-022-01625-y>
- Ciesla FJ (2007) Dust coagulation and settling in layered protoplanetary disks. *Astrophys J* 654:159–162
- Clark RN, Brown RH, Jaumann R et al (2005) Compositional maps of Saturn's moon Phoebe from imaging spectroscopy. *Nature* 435(7038):66–69. <https://doi.org/10.1038/nature03558>
- Combe JP, McCord TB, Tosi F et al (2016) Detection of local H₂O exposed at the surface of Ceres. *Science* 353(6303):aaf3010. <https://doi.org/10.1126/science.aaf3010>
- Crovisier J, Leech K, Bockelee-Morvan D et al (1997) The spectrum of comet Hale-Bopp (C/1995 O1) observed with the infrared space observatory at 2.9 astronomical units from the sun. *Science* 275:1904–1907. <https://doi.org/10.1126/science.275.5308.1904>
- Cruikshank DP, Roush TL, Bartholomew MJ et al (1998) The composition of centaur 5145 Pholus. *Icarus* 135(2):389–407. <https://doi.org/10.1006/icar.1998.5997>
- Cruikshank DP, Dalle Ore CM, Roush TL et al (2001) Constraints on the composition of Trojan asteroid 624 Hektor. *Icarus* 153(2):348–360. <https://doi.org/10.1006/icar.2001.6703>
- De Luise F, Dotto E, Fornasier S et al (2010) A peculiar family of Jupiter Trojans: the eurybates. *Icarus* 209(2):586–590. <https://doi.org/10.1016/j.icarus.2010.04.024>, arXiv:1004.4180 [astro-ph.EP]
- De Sanctis MC, Ammannito E, Raponi A et al (2015) Ammoniated phyllosilicates with a likely outer solar system origin on (1) Ceres. *Nature* 528(7581):241–244. <https://doi.org/10.1038/nature16172>
- De Sanctis MC, Capaccioni F, Ciarniello M et al (2015) The diurnal cycle of water ice on comet 67P/Churyumov-Gerasimenko. *Nature* 525(7570):500–503. <https://doi.org/10.1038/nature14869>
- De Sanctis MC, Ammannito E, McSween HY et al (2017) Localized aliphatic organic material on the surface of Ceres. *Science* 355(6326):719–722. <https://doi.org/10.1126/science.aaj2305>
- de Sanctis MC, Ammannito E, Carozzo FG et al (2018) Ceres's global and localized mineralogical composition determined by dawn's visible and infrared spectrometer (VIR). *Meteorit Planet Sci* 53(9):1844–1865. <https://doi.org/10.1111/maps.13104>
- De Sanctis MC, Ammannito E, Raponi A et al (2020) Fresh emplacement of hydrated sodium chloride on Ceres from ascending salty fluids. *Nat Astron* 4:786–793. <https://doi.org/10.1038/s41550-020-1138-8>
- Delsanti A, Peixinho N, Boehnhardt H et al (2006) Near-infrared color properties of Kuiper belt objects and centaurs: final results from the ESO large program. *Astron J* 131(3):1851–1863. <https://doi.org/10.1086/499402>

- DeMeo FE, Carry B (2013) The taxonomic distribution of asteroids from multi-filter all-sky photometric surveys. *Icarus* 226(1):723–741. <https://doi.org/10.1016/j.icarus.2013.06.027>. arXiv:1307.2424 [astro-ph.EP]
- DeMeo FE, Binzel RP, Carry B et al (2014) Unexpected D-type interlopers in the inner main belt. *Icarus* 229:392–399. <https://doi.org/10.1016/j.icarus.2013.11.026>. arXiv:1312.2962 [astro-ph.EP]
- Deshapriya JDP, Barucci MA, Fornasier S et al (2018) Exposed bright features on the comet 67P/Churyumov-Gerasimenko: distribution and evolution. *Astron Astrophys* 613:A36. <https://doi.org/10.1051/0004-6361/201732112>
- Dotto E, Fornasier S, Barucci MA et al (2006) The surface composition of Jupiter Trojans: visible and near-infrared survey of dynamical families. *Icarus* 183(2):420–434. <https://doi.org/10.1016/j.icarus.2006.02.012>
- Dotto E, Emery JP, Barucci MA et al (2008) De troianis: the Trojans in the planetary system. In: Barucci MA, Boehnhardt H, Cruikshank DP et al (eds) *The solar system beyond Neptune*. Univ Ariz Press, p 383
- Duffard R, Pinilla-Alonso N, Santos-Sanz P et al (2014) “TNOs are cool”: a survey of the trans-Neptunian region. XI. A Herschel-PACS view of 16 centaurs. *Astron Astrophys* 564:A92. <https://doi.org/10.1051/0004-6361/201322377>. arXiv:1309.0946 [astro-ph.EP]
- Dumas C, Owen T, Barucci MA (1998) Near-infrared spectroscopy of low-albedo surfaces of the solar system: search for the spectral signature of dark material. *Icarus* 133(2):221–232. <https://doi.org/10.1006/icar.1998.5927>
- Emery JP, Brown RH (2003) Constraints on the surface composition of Trojan asteroids from near-infrared (0.8–4.0 μm) spectroscopy. *Icarus* 164(1):104–121. [https://doi.org/10.1016/S0019-1035\(03\)00143-X](https://doi.org/10.1016/S0019-1035(03)00143-X)
- Emery JP, Brown RH (2004) The surface composition of Trojan asteroids: constraints set by scattering theory. *Icarus* 170(1):131–152. <https://doi.org/10.1016/j.icarus.2004.02.004>
- Emery JP, Cruikshank DP, Van Cleve J (2006) Thermal emission spectroscopy (5.2–38 μm) of three Trojan asteroids with the spitzer space telescope: detection of fine-grained silicates. *Icarus* 182(2):496–512. <https://doi.org/10.1016/j.icarus.2006.01.011>
- Emery JP, Burr DM, Cruikshank DP (2011) Near-infrared spectroscopy of Trojan asteroids: evidence for two compositional groups. *Astron J* 141(1):25. <https://doi.org/10.1088/0004-6256/141/1/25>. arXiv:1012.1284 [astro-ph.EP]
- Emery JP, Marzari F, Morbidelli A et al (2015) The Complex History of Trojan Asteroids. In: Michel P, DeMeo FE, Bottke WF (eds) *Asteroids IV*. University of Arizona Press, Tucson, pp 203–220. https://doi.org/10.2458/azu_uapress_9780816532131-ch011
- Farnham TL, Wellnitz DD, Hampton DL et al (2007) Dust coma morphology in the deep impact images of comet 9P/Tempel 1. *Icarus* 191(2 Suppl.):146–160. <https://doi.org/10.1016/j.icarus.2006.10.038>
- Feaga LM, A’Hearn MF, Sunshine JM et al (2007) Asymmetries in the distribution of H₂O and CO₂ in the inner coma of comet 9P/Tempel 1 as observed by Deep Impact. *Icarus* 190(2):345–356. <https://doi.org/10.1016/j.icarus.2007.04.009>
- Fernández YR, Jewitt DC, Sheppard SS (2001) Low albedos among extinct comet candidates. *Astrophys J Lett* 553(2):L197–L200. <https://doi.org/10.1086/320689>. arXiv:astro-ph/0104478 [astro-ph]
- Fernández YR, Sheppard SS, Jewitt DC (2003) The albedo distribution of Jovian Trojan asteroids. *Astron J* 126(3):1563
- Fernández YR, Jewitt D, Ziffer JE (2009) Albedos of small Jovian Trojans. *Astron J* 138(1):240–250. <https://doi.org/10.1088/0004-6256/138/1/240>. arXiv:0906.1786 [astro-ph.EP]
- Filacchione G, Raponi A, Capaccioni F et al (2016) Seasonal exposure of carbon dioxide ice on the nucleus of comet 67P/Churyumov-Gerasimenko. *Science* 354(6319):1563–1566. <https://doi.org/10.1126/science.aag3161>
- Fornasier S, Dotto E, Marzari F et al (2004) Visible spectroscopic and photometric survey of L5 Trojans: investigation of dynamical families. *Icarus* 172(1):221–232. <https://doi.org/10.1016/j.icarus.2004.06.015>
- Fornasier S, Dotto E, Hainaut O et al (2007) Visible spectroscopic and photometric survey of Jupiter Trojans: final results on dynamical families. *Icarus* 190(2):622–642. <https://doi.org/10.1016/j.icarus.2007.03.033>. arXiv:0704.0350 [astro-ph]
- Fornasier S, Mottola S, Keller HU et al (2016) Rosetta’s comet 67P/Churyumov-Gerasimenko sheds its dusty mantle to reveal its icy nature. *Science* 354(6319):1566–1570. <https://doi.org/10.1126/science.aag2671>
- Fornasier S, Hoang HV, Fulle M et al (2023) Volatile exposures on the 67P/Churyumov-Gerasimenko nucleus. *Astron Astrophys* 672:A136. <https://doi.org/10.1051/0004-6361/202245614>. arXiv:2302.11424 [astro-ph.EP]
- Frank D, Zolensky M, Le L (2014) Olivine in terminal particles of stardust aerogel tracks and analogous grains in chondrite matrix. *Geochim Cosmochim Acta* 142:240–259. <https://doi.org/10.1016/j.gca.2014.05.037>
- Fraser WC, Brown ME (2012) The Hubble wide field camera 3 test of surfaces in the outer solar system: the compositional classes of the Kuiper belt. *Astrophys J* 749(1):33. <https://doi.org/10.1088/0004-637X/749/1/33>. arXiv:1202.0827 [astro-ph.EP]

- Fraser WC, Brown ME (2018) Phoebe: a surface dominated by water. *Astron J* 156(1):23. <https://doi.org/10.3847/1538-3881/aac213>. arXiv:1803.04979 [astro-ph.EP]
- Fu X, Zou Y, Zheng Y et al (2012) Effects of space weathering on diagnostic spectral features: results from He⁺ irradiation experiments. *Icarus* 219(2):630–640. <https://doi.org/10.1016/j.icarus.2012.03.009>
- Gail HP, Sedlmayr E (1999) Mineral formation in stellar winds I. Condensation sequence of silicate and iron grains in stationary oxygen rich outflows. *Astron Astrophys* 347:594–616
- Gartrelle GM, Hardersen PS, Izawa MRM et al (2021) Illuminating the dark side of the asteroid population: visible near-infrared (0.7–2.45 μm) surface mineralogy modeling of D-type asteroids using Shkuratov theory. *Icarus* 354:114043. <https://doi.org/10.1016/j.icarus.2020.114043>
- Gradie J, Tedesco E (1982) Compositional structure of the asteroid belt. *Science* 216(4553):1405–1407. <https://doi.org/10.1126/science.216.4553.1405>
- Gradie J, Veverka J (1980) The composition of the Trojan asteroids. *Nature* 283(5750):840–842. <https://doi.org/10.1038/283840a0>
- Grav T, Mainzer AK, Bauer JM et al (2012) WISE/NEOWISE observations of the Jovian Trojan population: taxonomy. *Astrophys J* 759(1):49. <https://doi.org/10.1088/0004-637X/759/1/49>. arXiv:1209.1549 [astro-ph.EP]
- Graykowski A, Jewitt D (2018) Colors and shapes of the irregular planetary satellites. *Astron J* 155(4):184. <https://doi.org/10.3847/1538-3881/aab49b>. arXiv:1803.01907 [astro-ph.EP]
- Guilbert-Lepoutre A (2012) Survival of amorphous water ice on centaurs. *Astron J* 144(4):97. <https://doi.org/10.1088/0004-6256/144/4/97>
- Guilbert-Lepoutre A (2014) Survival of water ice in Jupiter Trojans. *Icarus* 231:232–238. <https://doi.org/10.1016/j.icarus.2013.12.014>. arXiv:1401.5196 [astro-ph.EP]
- Hanner MS, Lynch DK, Russell RW (1994) The 8–13 micron spectra of comets and the composition of silicate grains. *Astrophys J* 425:274–285
- Hapke B (1965) Effects of a simulated solar wind on the photometric properties of rocks and powders. *Ann NY Acad Sci* 123:711–721. <https://doi.org/10.1111/j.1749-6632.1965.tb20395.x>
- Hapke B (2001) Space weathering from Mercury to the asteroid belt. *J Geophys Res* 106(E5):10039–10074. <https://doi.org/10.1029/2000JE001338>
- Harker DE, Woodward CE, Wooden DH (2005) The dust grains from 9P/Tempel 1 before and after the encounter with Deep Impact. *Science* 310(5746):278–280. <https://doi.org/10.1126/science.1119143>
- Harker DE, Woodward CE, Wooden DH et al (2007) Gemini-N mid-IR observations of the dust properties of the ejecta excavated from comet 9P/Tempel 1 during Deep Impact. *Icarus* 190(2):432–453. <https://doi.org/10.1016/j.icarus.2007.03.008>
- Henning T (2010) Cosmic silicates. *Annu Rev Astron Astrophys* 48:21–46. <https://doi.org/10.1146/annurev-astro-081309-130815>
- Hiroi T, Zolensky ME, Pieters CM (2001) The Tagish Lake meteorite: a possible sample from a D-type asteroid. *Science* 293(5538):2234–2236. <https://doi.org/10.1126/science.1063734>
- Horner J, Evans NW, Bailey ME (2004) Simulations of the population of centaurs - I. The bulk statistics. *Mon Not R Astron Soc* 354(3):798–810. <https://doi.org/10.1111/j.1365-2966.2004.08240.x>. arXiv:astro-ph/0407400 [astro-ph]
- Horner J, Müller TG, Lykawka PS (2012) (1173) Anchises - thermophysical and dynamical studies of a dynamically unstable Jovian Trojan. *Mon Not R Astron Soc* 423(3):2587–2596. <https://doi.org/10.1111/j.1365-2966.2012.21067.x>. arXiv:1204.1388 [astro-ph.EP]
- Hughes AL, Armitage PJ (2010) Particle transport in evolving protoplanetary disks: implications for results from stardust. *Astrophys J* 719(2):1633–1653. <https://doi.org/10.1088/0004-637X/719/2/1633>. arXiv:1007.1989
- Humes OA, Thomas CA, Emery JP et al (2022) Ultraviolet spectroscopy of Lucy mission targets with the Hubble space telescope. *Planet Sci J* 3(8):190. <https://doi.org/10.3847/PSJ/ac8059>. arXiv:2207.11390 [astro-ph.EP]
- Izawa MR, King PL, Vernazza P et al (2021) Salt – a critical material to consider when exploring the solar system. *Icarus* 359(October 2020):114328. <https://doi.org/10.1016/j.icarus.2021.114328>
- Jäger C, Molster FJ, Dorschner J et al (1998) Steps toward interstellar silicate mineralogy IV. The crystalline revolution. *Astron Astrophys* 339:904–916
- Jewitt D (2009) The active centaurs. *Astron J* 137(5):4296–4312. <https://doi.org/10.1088/0004-6256/137/5/4296>. arXiv:0902.4687 [astro-ph.EP]
- Jewitt D (2015) Color systematics of comets and related bodies. *Astron J* 150(6):201. <https://doi.org/10.1088/0004-6256/150/6/201>. arXiv:1510.07069 [astro-ph.EP]
- Jewitt DC, Luu JX (1990) CCD spectra of asteroids. II - The Trojans as spectral analogs of cometary nuclei. *Astron J* 100:933–944. <https://doi.org/10.1086/115572>
- Kaňuchová Z, Baratta GA, Garozzo M et al (2010) Space weathering of asteroidal surfaces. Influence on the UV-Vis spectra. *Astron Astrophys* 517:A60. <https://doi.org/10.1051/0004-6361/201014061>

- Kaňuchová Z, Brunetto R, Melita M et al (2012) Space weathering and the color indexes of minor bodies in the outer solar system. *Icarus* 221(1):12–19. <https://doi.org/10.1016/j.icarus.2012.06.043>
- Kelley MS, Wooden DH (2009) The composition of dust in Jupiter-family comets inferred from infrared spectroscopy. *Planet Space Sci* 57(10):1133–1145. <https://doi.org/10.1016/j.pss.2008.11.017>
- Kelley MS, Woodward CE, Gehr RD et al (2017) Mid-infrared spectra of comet nuclei. *Icarus* 284:344–358. <https://doi.org/10.1016/j.icarus.2016.11.029>
- Koike C, Shibai H, Tsuchiyama A (1993) Extinction of olivine and pyroxene in the mid- and far-infrared. *Mon Not R Astron Soc* 264(3):654–658
- Koike C, Chihara H, Tsuchiyama A et al (2003) Compositional dependence of infrared absorption spectra of crystalline silicate II. Natural and synthetic olivines. *Astron Astrophys* 399(3):1101–1107. <https://doi.org/10.1051/0004-6361:20021831>
- Lamy PL, Toth I, Fernández YR et al (2004) The sizes, shapes, albedos, and colors of cometary nuclei. In: Festou MC, Keller HU, Weaver HA (eds) *Comets II*. University of Arizona Press, Tucson, pp 223–264
- Lantz C, Clark BE, Barucci MA et al (2013) Evidence for the effects of space weathering spectral signatures on low albedo asteroids. *Astron Astrophys* 554:A138. <https://doi.org/10.1051/0004-6361/201321593>
- Lantz C, Brunetto R, Barucci MA et al (2017) Ion irradiation of carbonaceous chondrites: a new view of space weathering on primitive asteroids. *Icarus* 285:43–57. <https://doi.org/10.1016/j.icarus.2016.12.019>
- Lazzarin M, Marchi S, Moroz LV et al (2006) Space weathering in the main asteroid belt: the big picture. *Astrophys J Lett* 647(2):L179–L182. <https://doi.org/10.1086/507448>
- Lazzaro D, Angeli CA, Carvano JM et al (2004) S³OS²: the visible spectroscopic survey of 820 asteroids. *Icarus* 172(1):179–220. <https://doi.org/10.1016/j.icarus.2004.06.006>
- Levison HF, Shoemaker EM, Shoemaker CS (1997) Dynamical evolution of Jupiter's Trojan asteroids. *Nature* 385:42–44
- Levison HF, Olkin CB, Noll KS et al (2021) Lucy mission to the Trojan asteroids: science goals. *Planet Sci J* 2(5):171. <https://doi.org/10.3847/PSJ/abf840>
- Licandro J, Pinilla-Alonso N (2005) The inhomogeneous surface of centaur 32522 Thereus (2001 PT₁₃). *Astrophys J Lett* 630(1):L93–L96. <https://doi.org/10.1086/491469>
- Lisse CM, VanCleve J, Adams AC et al (2006) Spitzer spectral observations of the deep impact ejecta. *Science* 313(5787):635–640. <https://doi.org/10.1126/science.1124694>
- Loeffler MJ, Baragiola RA, Murayama M (2008) Laboratory simulations of redeposition of impact ejecta on mineral surfaces. *Icarus* 196(1):285–292. <https://doi.org/10.1016/j.icarus.2008.02.021>
- Loeffler MJ, Dukes CA, Baragiola RA (2009) Irradiation of olivine by 4 keV He⁺: simulation of space weathering by the solar wind. *J Geophys Res, Planets* 114(E3):E03003. <https://doi.org/10.1029/2008JE003249>
- Lowry VC, Donaldson Hanna KL, Ito G et al (2022) T-matrix and Hapke modeling of the thermal infrared spectra of Trojan asteroids and (944) Hidalgo: implications for their regolith particle size and porosity. *Planet Sci J* 3(7):181. <https://doi.org/10.3847/PSJ/ac7a30>
- Luu J, Jewitt D, Cloutis E (1994) Near-infrared spectroscopy of primitive solar system objects. *Icarus* 109(1):133–144. <https://doi.org/10.1006/icar.1994.1081>
- Mahjoub A, Poston MJ, Hand KP et al (2016) Electron irradiation and thermal processing of mixed-ices of potential relevance to Jupiter Trojan asteroids. *Astrophys J* 820(2):141. <https://doi.org/10.3847/0004-637X/820/2/141>
- Mahjoub A, Poston MJ, Blacksborg J et al (2017) Production of sulfur allotropes in electron irradiated Jupiter Trojans ice analogs. *Astrophys J* 846(2):148. <https://doi.org/10.3847/1538-4357/aa85e0>
- Marchi S, Brunetto R, Magrin S et al (2005) Space weathering of near-Earth and main belt silicate-rich asteroids: observations and ion irradiation experiments. *Astron Astrophys* 443(3):769–775. <https://doi.org/10.1051/0004-6361:20053525>
- Marchi S, Bell JF, Bierhaus B et al (2023) Surface geology of Jupiter's Trojan asteroids. *Space Sci Rev* 219(5):44. <https://doi.org/10.1007/s11214-023-00985-9>
- Marsset M, Vernazza P, Gourgeot F et al (2014) Similar origin for low- and high-albedo Jovian Trojans and Hilda asteroids? *Astron Astrophys* 568:L7. <https://doi.org/10.1051/0004-6361/201424105>. arXiv:1407.7016 [astro-ph.EP]
- Martin AC (2022) Mid-infrared spectral studies of Jovian Trojan asteroids and the effects of regolith porosity. PhD thesis, Northern Arizona University. <https://www.proquest.com/dissertations-theses/mid-infrared-spectral-studies-Jovian-trojan/docview/2708280124/se-2>
- Martin AC, Emery JP (2023) MIR spectra and analysis of Jovian Trojan asteroids. *Planet Sci J* 4(8):153. <https://doi.org/10.3847/PSJ/aced0c>
- Martin AC, Emery JP, Loeffler MJ (2022) Spectral effects of regolith porosity in the mid-IR - forsteritic olivine. *Icarus* 378:114921. <https://doi.org/10.1016/j.icarus.2022.114921>
- Martin AC, Emery JP, Loeffler MJ (2023a) Spectral effects of regolith porosity in the mid-IR - pyroxene. *Icarus* 397:115507. <https://doi.org/10.1016/j.icarus.2023.115507>


- Martin AC, Emery JP, Wong I et al (2023b) JWST MIRI-MRS observations of Lucy's Trojan targets. In: Asteroids, comets, meteors 2023, p 2465
- Marzari F, Scholl H (1998) Capture of Trojans by a growing proto-Jupiter. *Icarus* 131:41–51
- McSween HY, Emery JP, Rivkin AS et al (2018) Carbonaceous chondrites as analogs for the composition and alteration of Ceres. *Meteorit Planet Sci* 53(9):1793–1804. <https://doi.org/10.1111/maps.12947>
- Melita MD, Licandro J, Jones DC et al (2008) Physical properties and orbital stability of the Trojan asteroids. *Icarus* 195(2):686–697. <https://doi.org/10.1016/j.icarus.2008.01.004>
- Melita MD, Strazzulla G, Bar-Nun A (2009) Collisions, cosmic radiation and the colors of the Trojan asteroids. *Icarus* 203(1):134–139. <https://doi.org/10.1016/j.icarus.2009.04.024>. arXiv:0906.4130 [astro-ph.EP]
- Melita MD, Kaňuchová Z, Brunetto R et al (2015) Space weathering and the color-color diagram of Plutinos and Jupiter Trojans. *Icarus* 248:222–229. <https://doi.org/10.1016/j.icarus.2014.09.050>
- Morbidelli A, Levison HF, Tsiganis K et al (2005) Chaotic capture of Jupiter's Trojan asteroids in the early solar system. *Nature* 435(7041):462–465. <https://doi.org/10.1038/nature03540>
- Morbidelli A, Brasser R, Tsiganis K et al (2009) Constructing the secular architecture of the solar system. I. The giant planets. *Astron Astrophys* 507(2):1041–1052. <https://doi.org/10.1051/0004-6361/200912876>
- Moroz LV, Fisenko AV, Semjonova LF et al (1996) Optical effects of regolith processes on S-asteroids as simulated by laser shots on ordinary chondrite and other mafic materials. *Icarus* 122(2):366–382. <https://doi.org/10.1006/icar.1996.0130>
- Mottola S, Hellmich S, Buie MW et al (2023) Shape models of Lucy targets (3548) Eurybates and (21900) Orus from disk-integrated photometry. *Planet Sci J* 4(1):18. <https://doi.org/10.3847/PSJ/acaf79>
- Mottola S, Britt D, Brown ME et al (2024) Shapes, rotations, photometric and internal properties of Jupiter Trojans. *Space Sci Rev* 220:17. <https://doi.org/10.1007/s11214-024-01052-7>
- Mueller M, Marchis F, Emery JP et al (2010) Eclipsing binary Trojan asteroid patrocclus: thermal inertia from spitzer observations. *Icarus* 205(2):505–515. <https://doi.org/10.1016/j.icarus.2009.07.043>. arXiv:0908.4198
- Müller T, Lellouch E, Fornasier S (2020) Trans-Neptunian objects and centaurs at thermal wavelengths. In: Prrialnik D, Barucci MA, Young L (eds) The trans-Neptunian solar system. Elsevier, Amsterdam, pp 153–181. <https://doi.org/10.1016/B978-0-12-816490-7.00007-2>
- Nesvorný D, Jedicke R, Whiteley RJ et al (2005) Evidence for asteroid space weathering from the sloan digital sky survey. *Icarus* 173(1):132–152. <https://doi.org/10.1016/j.icarus.2004.07.026>
- Nesvorný D, Vokrouhlický D, Morbidelli A (2013) Capture of Trojans by jumping Jupiter. *Astrophys J* 768(1):45. <https://doi.org/10.1088/0004-637X/768/1/45>. arXiv:1303.2900 [astro-ph.EP]
- Noll KS, Brown ME, Buie MW et al (2023) Trojan asteroid satellites, rings, and activity. *Space Sci Rev* 219(7):59. <https://doi.org/10.1007/s11214-023-01001-w>
- Oklay N, Mottola S, Vincent JB et al (2017) Long-term survival of surface water ice on comet 67P. *Mon Not R Astron Soc* 469:S582–S597. <https://doi.org/10.1093/mnras/stx2298>
- Olkin CB, Levison HF, Vincent M et al (2021) Lucy mission to the Trojan asteroids: instrumentation and encounter concept of operations. *Planet Sci J* 2(5):172. <https://doi.org/10.3847/PSJ/abf83f>. arXiv:2104.04575 [astro-ph.IM]
- O'Rourke L, Heinisch P, Blum J et al (2020) The Philae lander reveals low-strength primitive ice inside cometary boulders. *Nature* 586(7831):697–701. <https://doi.org/10.1038/s41586-020-2834-3>
- Owen TC, Cruikshank DP, Dalle Ore CM et al (1999) NOTE: detection of water ice on Saturn's satellite Phoebe. *Icarus* 139(2):379–382. <https://doi.org/10.1006/icar.1999.6116>
- Peixinho N, Doressoundiram A, Delsanti A et al (2003) Reopening the TNOs color controversy: centaurs bimodality and TNOs unimodality. *Astron Astrophys* 410:L29–L32. <https://doi.org/10.1051/0004-6361/20031420>. arXiv:astro-ph/0309428 [astro-ph]
- Peixinho N, Delsanti A, Guilbert-Lepoutre A et al (2012) The bimodal colors of centaurs and small Kuiper belt objects. *Astron Astrophys* 546:A86. <https://doi.org/10.1051/0004-6361/201219057>. arXiv:1206.3153 [astro-ph.EP]
- Peixinho N, Delsanti A, Doressoundiram A (2015) Reanalyzing the visible colors of centaurs and KBOs: what is there and what we might be missing. *Astron Astrophys* 577:A35. <https://doi.org/10.1051/0004-6361/201425436>. arXiv:1502.04145 [astro-ph.EP]
- Perna D, Barucci MA, Fulchignoni M et al (2018a) A spectroscopic survey of the small near-Earth asteroid population: peculiar taxonomic distribution and phase reddening. *Planet Space Sci* 157:82–95. <https://doi.org/10.1016/j.pss.2018.03.008>. arXiv:1803.08953
- Perna D, Bott N, Hromakina T et al (2018b) Rotationally-resolved spectroscopy of Jupiter Trojans (624) Hektor and (911) Agamemnon. *Mon Not R Astron Soc* 475(1):974–980. <https://doi.org/10.1093/mnras/stx3341>
- Pinilla-Alonso N, Popescu M, Licandro J et al (2022) Detection of the irregular shape of the southern limb of Menoetius from observations of the 2017–2018 Patroclus–Menoetius mutual events. *Planet Sci J* 3(12):267. <https://doi.org/10.3847/PSJ/ac9f11>

- Poch O, Istiqomah I, Quirico E et al (2020) Ammonium salts are a reservoir of nitrogen on a cometary nucleus and possibly on some asteroids. *Science* 367(6483):aaw7462. <https://doi.org/10.1126/science.aaw7462>. [arXiv:2003.06034](https://arxiv.org/abs/2003.06034) [astro-ph.EP]
- Pommerol A, Thomas N, El-Maarry MR et al (2015) OSIRIS observations of meter-sized exposures of H₂O ice at the surface of 67P/Churyumov-Gerasimenko and interpretation using laboratory experiments. *Astron Astrophys* 583:A25. <https://doi.org/10.1051/0004-6361/201525977>
- Porco CC, Baker E, Barbara J et al (2005) Cassini imaging science: initial results on Phoebe and Iapetus. *Science* 307(5713):1237–1242. <https://doi.org/10.1126/science.1107981>
- Poston MJ, Mahjoub A, Ehlmann BL et al (2018) Visible near-infrared spectral evolution of irradiated mixed ices and application to Kuiper belt objects and Jupiter Trojans. *Astrophys J* 856(2):124. <https://doi.org/10.3847/1538-4357/aab1f1>
- Prialnik D, Brosch N, Ianovici D (1995) Modelling the activity of 2060 Chiron. *Mon Not R Astron Soc* 276(4):1148–1154. <https://doi.org/10.1093/mnras/276.4.1148>
- Quirico E, Moroz LV, Schmitt B et al (2016) Refractory and semi-volatile organics at the surface of comet 67P/Churyumov-Gerasimenko: insights from the VIRTIS/Rosetta imaging spectrometer. *Icarus* 272:32–47. <https://doi.org/10.1016/j.icarus.2016.02.028>
- Raponi A, Ciarniello M, Capaccioni F et al (2020) Infrared detection of aliphatic organics on a cometary nucleus. *Nat Astron* 4:500–505. <https://doi.org/10.1038/s41550-019-0992-8>. [arXiv:2009.14476](https://arxiv.org/abs/2009.14476) [astro-ph.EP]
- Reuter DC, Simon AA, Lunsford A et al (2023) L’Ralph: a visible/infrared spectral imager for the Lucy mission to the Trojans. *Space Sci Rev* 219(8):69. <https://doi.org/10.1007/s11214-023-01009-2>
- Ribeiro de Sousa R, Morbidelli A, Gomes R et al (2022) Dynamical origin of the dwarf planet Ceres. *Icarus* 379:114933. <https://doi.org/10.1016/j.icarus.2022.114933>, [arXiv:2202.09238](https://arxiv.org/abs/2202.09238) [astro-ph.EP]
- Rivkin AS, Emery JP, Howell ES et al (2022) The nature of low-albedo small bodies from 3 μ m spectroscopy: one group that formed within the ammonia snow line and one that formed beyond it. *Planet Sci J* 3(7):153. <https://doi.org/10.3847/PSJ/ac7217>. [arXiv:2205.09166](https://arxiv.org/abs/2205.09166) [astro-ph.EP]
- Roig F, Ribeiro AO, Gil-Hutton R (2008) Taxonomy of asteroid families among the Jupiter Trojans: comparison between spectroscopic data and the sloan digital sky survey colors. *Astron Astrophys* 483(3):911–931. <https://doi.org/10.1051/0004-6361:20079177>. [arXiv:0712.0046](https://arxiv.org/abs/0712.0046) [astro-ph]
- Romanishin W, Tegler SC (2018) Albedos of centaurs, Jovian Trojans, and Hildas. *Astron J* 156(1):19. <https://doi.org/10.3847/1538-3881/aac210>
- Romon-Martin J, Delahodde C, Barucci MA et al (2003) Photometric and spectroscopic observations of (2060) Chiron at the ESO Very Large Telescope. *Astron Astrophys* 400:369–373. <https://doi.org/10.1051/0004-6361:20021890>
- Roush T (2003) Estimated optical constants of the Tagish Lake meteorite. *Meteorit Planet Sci* 38(3):419–426. <https://doi.org/10.1111/j.1945-5100.2003.tb00277.x>
- Sasaki S, Nakamura K, Hamabe Y et al (2001) Production of iron nanoparticles by laser irradiation in a simulation of lunar-like space weathering. *Nature* 410(6828):555–557
- Schaller EL, Brown ME (2007) Volatile loss and retention on Kuiper belt objects. *Astrophys J Lett* 659(1):L61–L64. <https://doi.org/10.1086/516709>
- Schwamb ME, Fraser WC, Bannister MT et al (2019) Col-OSSOS: the colors of the outer solar system origins survey. *Astrophys J Suppl Ser* 243(1):12. <https://doi.org/10.3847/1538-4365/ab2194>. [arXiv:1809.08501](https://arxiv.org/abs/1809.08501) [astro-ph.EP]
- Simpson AM, Brown ME, Schemel MJ et al (2022) An ALMA search for high-albedo objects among the mid-sized Jupiter Trojan population. *Astron J* 164(1):23
- Slyusarev IG, Belskaya IN (2014) Jupiter’s Trojans: physical properties and origin. *Sol Syst Res* 48(2):139–157. <https://doi.org/10.1134/S0038094614020063>
- Souza-Feliciano AC, De Prá M, Pinilla-Alonso N et al (2020) Analysis in the visible range of NASA Lucy mission targets: Eurybates, Polymele, Orus and Donaldjohanson. *Icarus* 338:113463. <https://doi.org/10.1016/j.icarus.2019.113463>, [arXiv:1907.11451](https://arxiv.org/abs/1907.11451) [astro-ph.EP]
- Stansberry J, Grundy W, Brown M et al (2008) Physical properties of Kuiper belt and centaur objects: constraints from the spitzer space telescope. In: Barucci MA, Boehnhardt H, Cruikshank DP et al (eds) *The solar system beyond Neptune*. University of Arizona Press, Tucson, p 161
- Steckloff JK, Lisse CM, Safrit TK et al (2021) The sublimative evolution of (486958) Arrokoth. *Icarus* 356:113998. <https://doi.org/10.1016/j.icarus.2020.113998>, [arXiv:2007.12657](https://arxiv.org/abs/2007.12657) [astro-ph.EP]
- Strazzulla G, Dotto E, Binzel R et al (2005) Spectral alteration of the Meteorite Epinal (H5) induced by heavy ion irradiation: a simulation of space weathering effects on near-Earth asteroids. *Icarus* 174(1):31–35. <https://doi.org/10.1016/j.icarus.2004.09.013>
- Sugita S, Ootsubo T, Kadono T et al (2005) Subaru telescope observations of deep impact. *Science* 310(5746):274–278. <https://doi.org/10.1126/science.1119091>

- Sunshine JM, A'Hearn MF, Groussin O et al (2006) Exposed water ice deposits on the surface of comet 9P/Tempel 1. *Science* 311(5766):1453–1455. <https://doi.org/10.1126/science.1123632>
- Szabó GM, Ivezić Ž, Jurić M et al (2007) The properties of Jovian Trojan asteroids listed in SDSS moving object catalogue 3. *Mon Not R Astron Soc* 377(4):1393–1406. <https://doi.org/10.1111/j.1365-2966.2007.11687.x>. arXiv:astro-ph/0703026 [astro-ph]
- Tegler S, Consolmagno G, Romanishin W (2006) Comet 174P/Echeclus. *IAU Circ* 8701:1
- Tegler SC, Romanishin W, Consolmagno GJ (2003) Color patterns in the Kuiper belt: a possible primordial origin. *Astrophys J Lett* 599(1):L49–L52. <https://doi.org/10.1086/381076>
- Tegler SC, Bauer JM, Romanishin W et al (2008) Colors of centaurs. In: Barucci MA, Boehnhardt H, Cruikshank DP et al (eds) *The solar system beyond Neptune*. University of Arizona Press, Tucson, p 105
- Tegler SC, Romanishin W, Consolmagno GJ et al (2016) Two color populations of Kuiper belt and centaur objects and the smaller orbital inclinations of red centaur objects. *Astron J* 152(6):210. <https://doi.org/10.3847/0004-6256/152/6/210>
- Tielens AGGM, Waters LBFM, Molster FJ et al (1998) Circumstellar silicate mineralogy. *Astrophys Space Sci* 255:415–426. <https://doi.org/10.1023/A:1001585120472>
- Tiscareno MS, Malhotra R (2003) The dynamics of known Centaurs. *Astron J* 126(6):3122–3131. <https://doi.org/10.1086/379554>, arXiv:astro-ph/0211076 [astro-ph]
- Tsiganis K, Gomes R, Morbidelli A et al (2005) Origin of the orbital architecture of the giant planets of the solar system. *Nature* 435(7041):459–461. <https://doi.org/10.1038/nature03539>
- Vernazza P, Delbo M, King PL et al (2012) High surface porosity as the origin of emissivity features in asteroid spectra. *Icarus* 221(2):1162–1172. <https://doi.org/10.1016/j.icarus.2012.04.003>
- Vernazza P, Fulvio D, Brunetto R et al (2013) Paucity of Tagish Lake-like parent bodies in the Asteroid Belt and among Jupiter Trojans. *Icarus* 225(1):517–525. <https://doi.org/10.1016/j.icarus.2013.04.019>
- Vilas F, Larson SM, Hatch EC et al (1993) CCD reflectance spectra of selected asteroids. II. Low-albedo asteroid spectra and data extraction techniques. *Icarus* 105(1):67–78. <https://doi.org/10.1006/icar.1993.1111>
- Watanabe JI (2004) Meteor streams and comets. *Earth Moon Planets* 95(1-4):49–61. <https://doi.org/10.1007/s11038-005-9045-7>
- Weaver HA, Wilson JP, Conard SJ et al (2023) The Lucy Long Range Reconnaissance Imager (L'LORRI). *Space Sci Rev* 219(8):82. <https://doi.org/10.1007/s11214-023-01028-z>
- Wong I, Brown ME (2015) The color-magnitude distribution of small Jupiter Trojans. *Astron J* 150(6):174. <https://doi.org/10.1088/0004-6256/150/6/174>. arXiv:1510.03144 [astro-ph.EP]
- Wong I, Brown ME (2016) A hypothesis for the color bimodality of Jupiter Trojans. *Astron J* 152(4):90. <https://doi.org/10.3847/0004-6256/152/4/90>. arXiv:1607.04133 [astro-ph.EP]
- Wong I, Brown ME (2017a) The bimodal color distribution of small Kuiper belt objects. *Astron J* 153(4):145. <https://doi.org/10.3847/1538-3881/aa60c3>. arXiv:1702.02615 [astro-ph.EP]
- Wong I, Brown ME (2017b) The color-magnitude distribution of Hilda asteroids: comparison with Jupiter Trojans. *Astron J* 153(2):69. <https://doi.org/10.3847/1538-3881/153/2/69>. arXiv:1701.00367 [astro-ph.EP]
- Wong I, Brown ME, Emery JP (2014) The differing magnitude distributions of the two Jupiter Trojan color populations. *Astron J* 148(6):112. <https://doi.org/10.1088/0004-6256/148/6/112>. arXiv:1408.2485 [astro-ph.EP]
- Wong I, Brown ME, Blacksborg J et al (2019a) Hubble ultraviolet spectroscopy of Jupiter Trojans. *Astron J* 157(4):161. <https://doi.org/10.3847/1538-3881/ab0e00>. arXiv:1903.03576 [astro-ph.EP]
- Wong I, Mishra A, Brown ME (2019b) Photometry of active centaurs: colors of dormant active centaur nuclei. *Astron J* 157(6):225. <https://doi.org/10.3847/1538-3881/ab1b22>. arXiv:1904.09255 [astro-ph.EP]
- Wong I, Brown M, Emery J et al (2023) JWST observations of the Lucy flyby targets: new spectroscopic constraints on Jupiter Trojan composition. In: *Asteroids, Comets, Meteors Conference 2023*, p 2556
- Wooden DH (2002) Comet grains: their IR emission and their relation to ISM grains. *Earth Moon Planets* 89(1):247–287. <https://doi.org/10.1023/A:1021515023679>
- Wooden DH (2008) Cometary refractory grains: interstellar and nebular sources. *Space Sci Rev* 138:75–108. <https://doi.org/10.1007/s11214-008-9424-2>
- Wooden DH, Woodward CE, Harker DE (2004) Discovery of crystalline silicates in comet C/2001 Q4 (NEAT). *Astrophys J* 612(1):L77–L80. <https://doi.org/10.1086/424593>
- Woodward CE, Kelley MSP, Harker DE et al (2015) SOFIA infrared spectrophotometry of comet C/2012 K1 (Pan-STARRS). *Astrophys J* 809(2):181. <https://doi.org/10.1088/0004-637X/809/2/181>. arXiv:1508.00288 [astro-ph.EP]
- Yang B, Jewitt D (2007) Spectroscopic search for water ice on Jovian Trojan asteroids. *Astron J* 134(1):223–228. <https://doi.org/10.1086/518368>
- Yang B, Lucey P, Glotch T (2013) Are large Trojan asteroids salty? An observational, theoretical, and experimental study. *Icarus* 223(1):359–366. <https://doi.org/10.1016/j.icarus.2012.11.025>. arXiv:1211.3099

Publisher's Note Springer Nature remains neutral with regard to jurisdictional claims in published maps and institutional affiliations.

Authors and Affiliations

Joshua P. Emery¹  · Richard P. Binzel² · Daniel T. Britt³ · Michael E. Brown⁴ · Carly J.A. Howett^{5,6} · Audrey C. Martin³ · Mario D. Melita^{7,8} · Ana Carolina Souza-Feliciano^{3,9} · Ian Wong¹⁰

✉ J.P. Emery
joshua.emery@nau.edu

- ¹ Northern Arizona University, Flagstaff, AZ, USA
- ² Massachusetts Institute of Technology, Cambridge, MA, USA
- ³ University of Central Florida, Orlando, FL, USA
- ⁴ California Institute of Technology, Pasadena, CA, USA
- ⁵ University of Oxford, Oxford, UK
- ⁶ Planetary Science Institute, Tucson, AZ, USA
- ⁷ CONICET-Universidad de Buenos Aires, Buenos Aires, Argentina
- ⁸ Universidad Nacional de La Plata, La Plata, Argentina
- ⁹ Florida Space Institute, Orlando, FL, USA
- ¹⁰ NASA Goddard Space Flight Center, Greenbelt, MD, USA